

2006

# Transverse drainages, divides and landscape evolution in the Great Valley, Eastern United States

Sarah Flanagan  
*Lehigh University*

Follow this and additional works at: <http://preserve.lehigh.edu/etd>

---

## Recommended Citation

Flanagan, Sarah, "Transverse drainages, divides and landscape evolution in the Great Valley, Eastern United States" (2006). *Theses and Dissertations*. Paper 914.

This Thesis is brought to you for free and open access by Lehigh Preserve. It has been accepted for inclusion in Theses and Dissertations by an authorized administrator of Lehigh Preserve. For more information, please contact [preserve@lehigh.edu](mailto:preserve@lehigh.edu).

Flanagan, Sarah  
Marguerite

Transverse  
Drainages,  
Divides and  
Landscape  
Evolution in the  
Great Valley...

January 2006

**Transverse drainages, divides and landscape evolution in the Great Valley, eastern  
United States**

By

Sarah Marguerite Flanagan

A Thesis

Presented to the Graduate and Research Committee

of Lehigh University

in Candidacy for the Degree of

Master of Science

in

Earth and Environmental Science

Lehigh University

This thesis is accepted and approved in partial fulfillment of the requirements for the Master of Science.

06 Dec 2005

Date

Dr. Frank J. Pazzaglia

---

Dr. Noel Potter Jr.

---

Dr. Joan M. Ramage

---

Dr. Peter K. Zeitler

## Acknowledgements

There are many people who helped me to complete this thesis. Firstly, I would like to thank my advisor, Frank J. Pazzaglia for his guidance and never ending patience. I would also like to thank my committee members, Noel Potter Jr. and Joan Ramage. Noel was a great help especially during the field portion of this project. Joan was always available to listen and ready with helpful suggestions. Other members of the EES department I would like to thank are Nancy Roman and Laura Cambiotti, without them, nothing would ever get done.

My family, as always, has been very supportive through this process and I would like to thank my Mother, Grandmother and Brother. Everyone needs a little quiet, fuzzy support and for that I always turn to my pets; Homer, Mattie, Phineas, Percy, Jack and in their absence Fred and Enzo.

Finally, the people who heard all the moaning a groaning as well as the off color jokes. I would like to thank my fellow graduate students in the EES department. I could have never gotten through my two and a half years at Lehigh without you. I need to give a special thanks to my officemates Jen Wollenberg, Sandi Connelly and Karina Walker (Honorary) and I would like to remind them to look inside the filing cabinet.

## Table of Contents

	Page Number
List of Tables	v
List of Figures	vi
Abstract	1
Introduction	2
<i>Study Area</i>	7
Base Level and Experimental Design	12
<i>DEM Analyses</i>	15
<i>Field Analyses</i>	22
Results	24
<i>Field-based Observations</i>	24
<i>Map-based Metrics</i>	32
<i>Longitudinal Profile Modeling</i>	35
Discussion	45
<i>Upland gravel and origin of the current drainage divide</i>	45
<i>Mobility of the drainage divide inferred from stream long profiles</i>	47
Conclusions	52
References	55
Appendix A – Upland Gravel Data	60
Vita	69

## List of Tables

	Page Number
Table 1 – Drainage Density Values	33
Table 2 – Mean Hypsometric Values	33
Table 3 – Longitudinal Profile Modeling Values	38
Table 4 - Longitudinal Profile Modeling Comparison Values	40

## List of Figures

	Page Number
Figure 1 – The Eastern United States	4
Figure 2 – Digital Elevation Model of the Great Valley	5
Figure 3 – Simplified Geologic Map of the Great Valley	9
Figure 4 – Stratigraphic Column of the Cumberland Valley	10
Figure 5 – Theoretical Cartoon of Longitudinal Profile Modeling	18
Figure 6 – Method of Longitudinal Profile Modeling	20
Figure 7 – Small Map of Cumberland Valley Cobbles	25
Figure 8 – Flinn Diagrams	27
Figure 9 – Weathering Rinds	28
Figure 10 – Rind Thickness Boxplot	29
Figure 11 – Thin Sections	31
Figure 12 – Hypsometric Interval Curves	34
Figure 13 – Distribution of Slope Values	36
Figure 14 – LogArea – LogSlope plot for all Streams	41
Figure 15 – LogArea – LogSlope plot for Shale Streams	43
Figure 16 – Schematic of Future Landscape Evolution	54



## **Abstract**

The processes controlling landscape evolution in the Great Valley, eastern United States is a controversial topic. The Great Valley was used to test two paradigms of landscape evolution; dynamic equilibrium (Hack, 1960) where the relief of the landscape remains constant even if there are changes in total elevation or position and that of W. M. Davis (Davis, 1889, 1899), which explained a landscape in slow decay from high relief to a peneplain that grades gently to base level. This study proposes to rectify these two apparently opposing paradigms using the landscape of the Great Valley. Consistent lithologic patterns for the Great Valley lead to consistent drainage patterns for each basin in the Great Valley. Generally, each basin has two major drainages that trend parallel to the strike of the Great Valley, one in the carbonates and one in the shales. These strike parallel drainages flow into one of the major rivers that transversely cut the Great Valley; the James, Potomac, Susquehanna and Delaware Rivers. Using several different methodological approaches; a field study, extraction of whole basin metrics from digital elevation models and longitudinal profile modeling, this study has reached several general conclusions about landscape evolution in the Great Valley. One, upland gravel deposits do not indicate watershed expansion. Two, channel metrics suggest systems in disequilibrium that are sluggishly connected to changes in base level. Three, the two southernmost basins in the study, between the James and Potomac rivers, show higher longitudinal profile modeling values than the other basin in the study. Four, ultimately, longitudinal profiling in this low slope environment proved to be insensitive.

## **Introduction**

There are many different conceptual paradigms on how landscapes evolve over long, geologic time scales. Two of the leading paradigms, those of J.T. Hack (1960) and W. M. Davis (1889, 1899), are generally viewed as incompatible, yet both were conceived to explain the landscape of the eastern United States. Hack (1960) argues that the Appalachian landscape is in or near a state of dynamic equilibrium which holds that relief within the overall landscape remains relatively constant, reflecting a characteristic balance between driving (climatic, tectonic) and resisting (rock-type, structure) forces. Alternatively, the Davisian model states that landscapes are first born by impulsive uplift, rapidly develop their maximum relief, and then progressively decay to a peneplain. This study seeks to understand several aspects of long term landscape evolution in the Appalachian Mountains in the context of these long-standing geomorphic paradigms, including the act of drainage self organization whereby drainages change from flowing consequent to topographic slope to flowing subsequent to structure and rock type. Both of these paradigms may describe the Appalachian landscape well for different temporal and spatial scales but both clearly predict that the erosional response of the landscape to the tectonic processes that constructed it in the first place is both long and complex. For the case of the Appalachians, an orogen built throughout the Paleozoic, the current landscape represents at least 200 Ma of erosional decay, arguably punctuated by post-orogenic epeirogeny (Pazzaglia and Brandon, 1996). The presence of relief and mountainous topography over this protracted decay period argues for surficial processes acting slowly and a sluggish linkage between tectonic processes and the subsequent

erosional response (Schumm and Rea, 1995), a conclusion supported by thermochronologic data (Hulver, 1992, 1996; Laucks, unpublished data).

Embedded within the central Appalachian Mountains are distinct physiographic provinces (fig. 1), each with a characteristic relief and topography dictated by the underlying rock-type and structure. The Great Valley is one of these physiographic provinces noteworthy of several core observations. First, it trends from the Hudson Valley in New York State through New Jersey, Pennsylvania, and Maryland to its southern end in Virginia and North Carolina. It has many local names including the Hudson Valley, Minsi Valley, Lehigh Valley, Cumberland Valley and Shenandoah Valley, respectively over its length. The Great Valley is underlain by distinct, continuous belts of Cambro-Ordovician siliciclastic and carbonate rocks. Second, drainage in the Great Valley is characteristically composed of long, strike parallel trellis channels developed independently on the carbonate and siliciclastic rocks (fig. 2). These strike parallel drainages, are each tributary to large, north-west to south-east flowing orogen-transverse rivers, such as the Susquehanna, Potomac, and James rivers, that drain the Appalachians at approximately regular 100 km intervals. Hack (1982) and Braun (1983) argued that strike parallel drainages in the Great Valley seemed to be well adjusted to rock type and the presence of upland gravels (see point three below) and supported the idea of inverted topography in the drainage of the Potomac River (Jacobsen, 1982). Third, the drainage divides at the head of the opposing strike-parallel drainages are asymmetric and locally mantled by upland gravels of diverse texture and composition. Qualitatively, differences in topography in the divide regions particularly exist between northern and southern parts of the Great Valley, which indicate fundamental differences

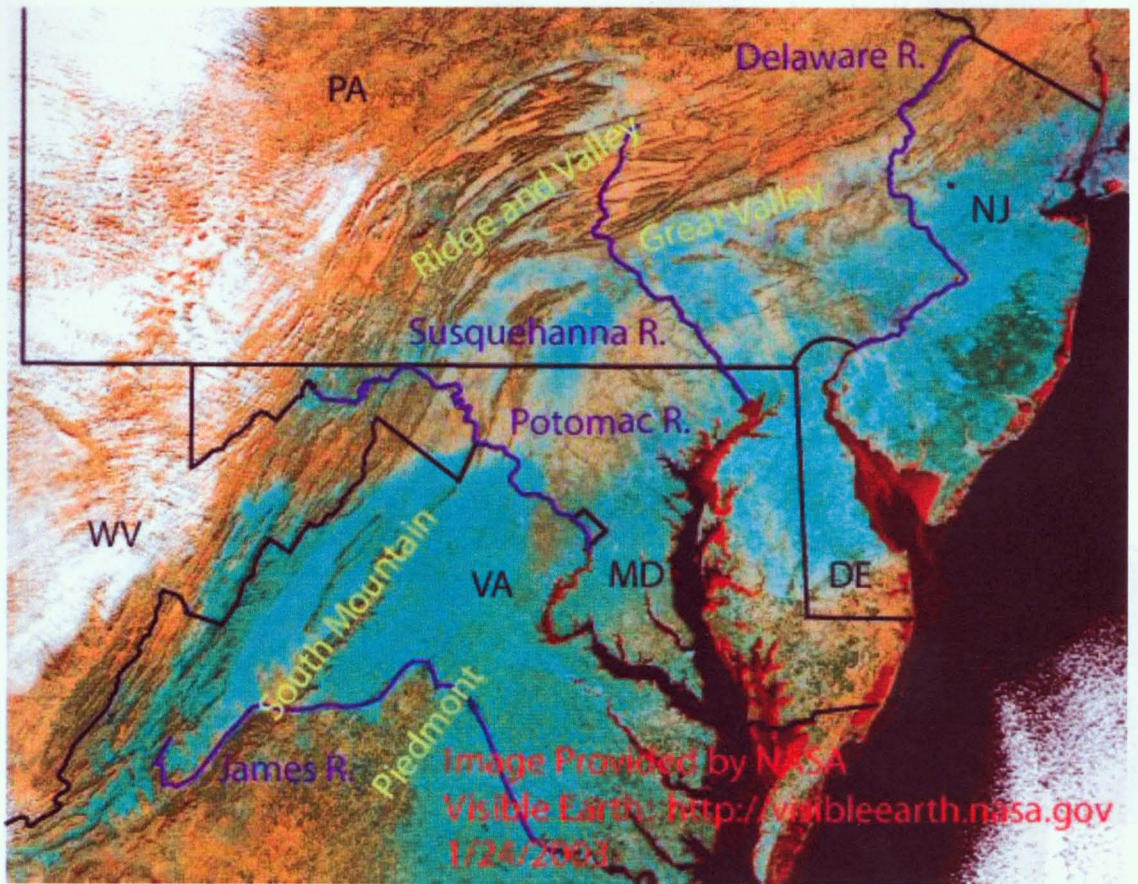


Figure 1. A satellite image of the eastern United States, the physiographic provinces are labeled including the Ridge and Valley, Great Valley, and Piedmont. The major transverse rivers draining the Great Valley and Ridge and Valley are shown in blue. Image provided by NASA, Visible Earth <http://visibleearth.nasa.gov>, 01/26/2003 in their erosional histories.

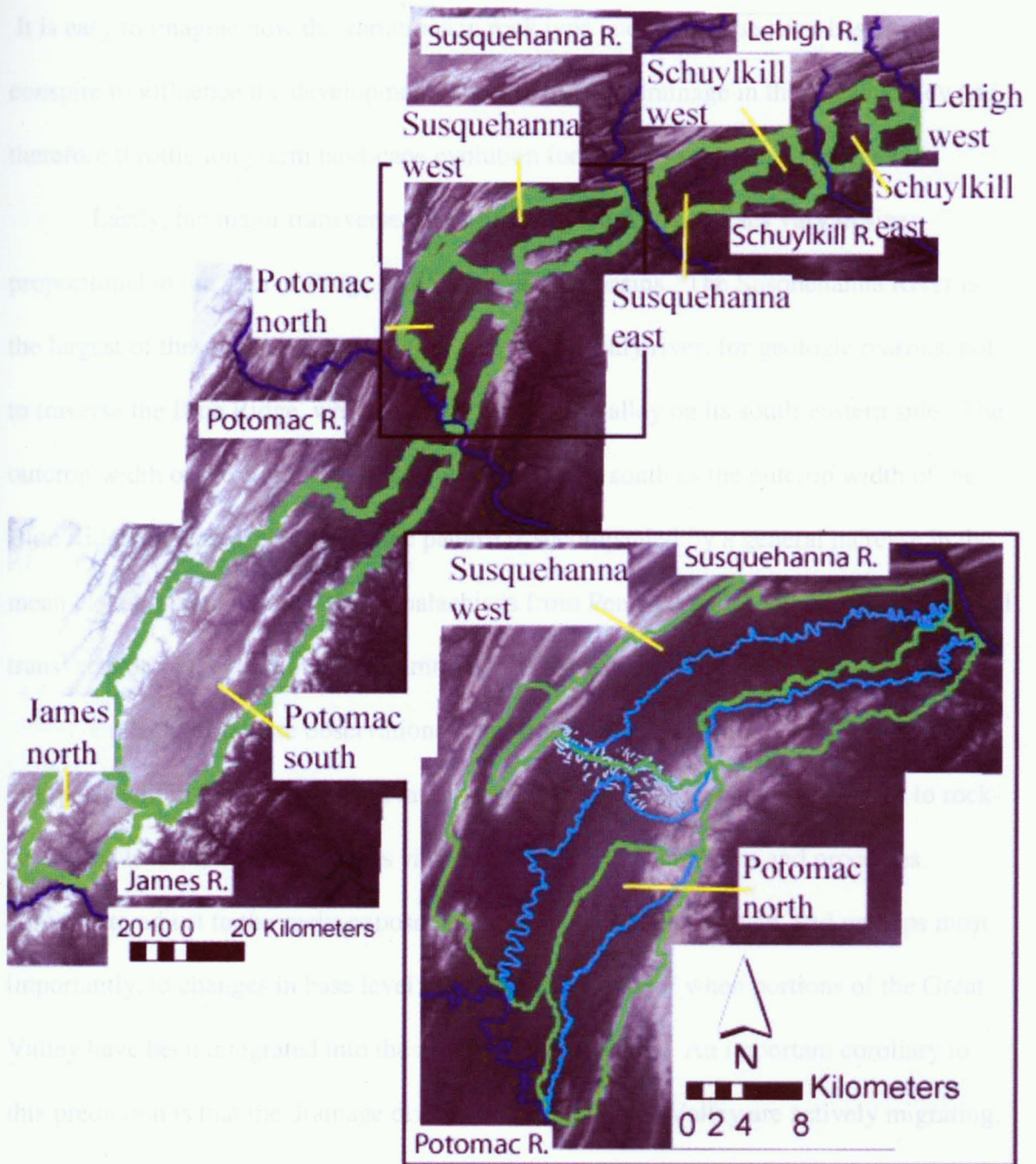


Figure 2. A Digital Elevation Model (DEM) of the Great Valley, with an inset showing a more detailed view of the Cumberland Valley. Major transverse rivers are labeled and shown in blue in both maps. Drainage basins are outlined in green. The inset shows the four drainage basins of the Cumberland Valley with the strike parallel streams in blue and the first order streams flanking the divide in the lightest shade of blue.

It is easy to imagine how the variations in rock type and transverse river base level conspire to influence the development of strike-parallel drainage in the Great Valley and therefore throttle long term landscape evolution for this physiographic province.

Lastly, the major transverse rivers draining the Appalachians vary in size proportional to the area of Ridge and Valley in their basins. The Susquehanna River is the largest of these transverse drainages and it is the only river, for geologic reasons, not to traverse the Blue Ridge, which borders the Great Valley on its south-eastern side. The outcrop width of the Ridge and Valley narrows to the south as the outcrop width of the Blue Ridge increases. This geologic pattern is accompanied by a general increase in the mean elevation and relief of the Appalachians from Pennsylvania south into Virginia. All transverse drainages respond to a common base level controlled by the Atlantic Ocean.

Collectively, these observations suggest that the Great Valley, and the strike drainages within it, reflect modern landforms all in a state of delicate adjustment to rock-type, base level, and climate. This view predicts that the landforms and processes continue to adjust to the rocks exposed to erosion, changes in climate, and perhaps most importantly, to changes in base level related to the timing of when portions of the Great Valley have been integrated into the main transverse rivers. An important corollary to this prediction is that the drainage divides within the Great Valley are actively migrating, rather than static features. A specific prediction made by this hypothesis is that drainage divides in the southern Great Valley should be steeper and more asymmetric than those in the north because integration of the James River into the Great Valley has been retarded by the wide, high Blue Ridge, an impediment progressively lacking for the northern Great Valley.

The alternative hypothesis is that the landforms and drainages of the Great Valley are relict features, more closely related to the proposed episodic beveling of the Appalachian topography (Davis, 1889, 1899) and or large changes in climate. The latter view predicts that the Great Valley landforms and processes are completely out of phase with modern surficial processes and a measure of disequilibrium in both form and process would support the Davisian, rather than Hackian paradigm for landscape evolution. A specific prediction of the disequilibrium hypothesis is that Great Valley divides are relatively static and show no discernable trends in steepness or asymmetry from north to south.

This thesis presents several field and laboratory experiments designed to test these hypotheses and determine which prediction better fits the observations. In the process, new methods for modeling the longitudinal profiles of rivers (Snyder, et al., 2000; Whipple, 2004) have been developed and a largely field-based sedimentologic data set has been merged with a largely DEM-topography based GIS analysis. The resulting synthesis favors a landscape undergoing constant, slow change that is not controlled by the timing of drainage integration to the master transverse drainages but rather by careful local adjustment to rock type and climate.

### *Study Area*

The Great Valley in Pennsylvania, Maryland, and northern Virginia, along with the Blue Ridge, lies in the footwall of Mesozoic normal faults that formed during the opening of the Atlantic Ocean in the late Triassic and early Jurassic. The footwall was presumably high standing during the Mesozoic, but tens of millions of years of

weathering and carbonate dissolution lead to an inverted topography where Great Valley rocks are now low-standing with respect to the Blue Ridge and Mesozoic basins. The presence of late Cretaceous lignites preserved in sinkholes at Pond Bank provide some constraints of when this topographic inversion occurred (Pierce, 1965), but reconstruction of a Cretaceous topography remains impossible. Since the Cretaceous, Great Valley landscape evolution has been dominated by mechanical denudation of the siliciclastics and dissolution of the carbonates which may or may not be proceeding at similar rates (Hack, 1960). Atlantic slope streams traverse the Great Valley more or less orthogonally and their size is proportional to the outcrop width of the Blue Ridge rocks that border the Great Valley to the east. The Great Valley lies an equal distance upstream from the Atlantic Ocean along these transverse drainages so the influence of Atlantic Ocean base level can be considered more or less the same throughout the study area.

The Great Valley is underlain of a band of shale on its north and west part and carbonate on the south and east part (fig. 3). The shale belt is characterized by sinuous channels while the carbonate is characterized by intermittent, gaining and losing streams. Sandstone/quartzite ridges bound each side of the Great Valley. The south and east is flanked by the Antietam Quartzite, which is a slightly metamorphosed, mature quartz sandstone with both carbonate and silica cement (fig. 4). On the north and west flank the Great Valley is bound by the Ordovician Bald Eagle Sandstone, Juniata Shale and the Silurian Tuscarora Sandstone. The Bald Eagle Sandstone is a sublitharenite with coarse, subangular, commonly olive-colored grains, whereas the Tuscarora Sandstone is a hard quartz arenite with rounded grains and silica cement. Streams carrying sandstone detritus



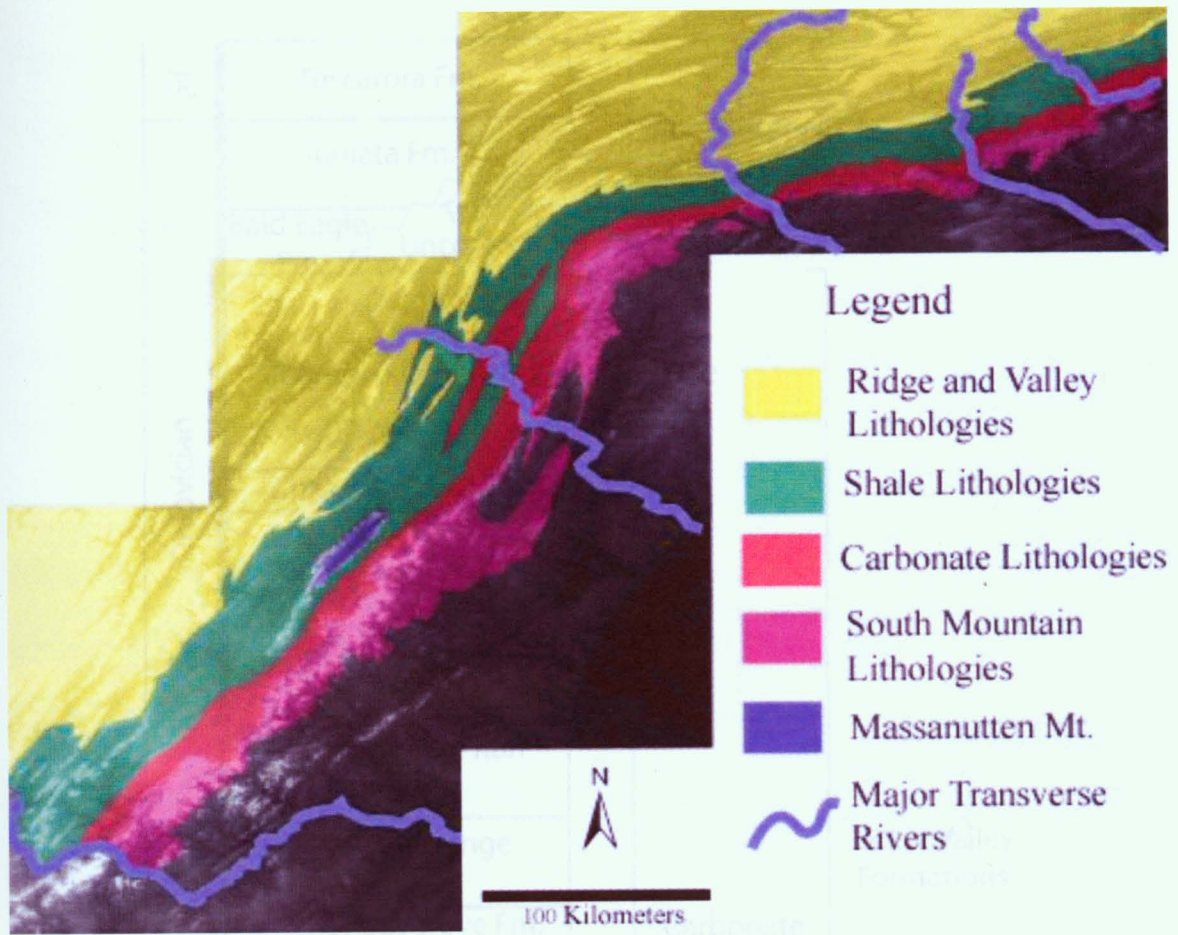


Figure 3. A simplified geologic map of the Great Valley overlain on a DEM. Rock types have been simplified to show South Mountain lithologies as one unit, Great Valley carbonates as one unit, Great Valley shales as one unit and the lithologies of the Valley and Ridge as one unit.

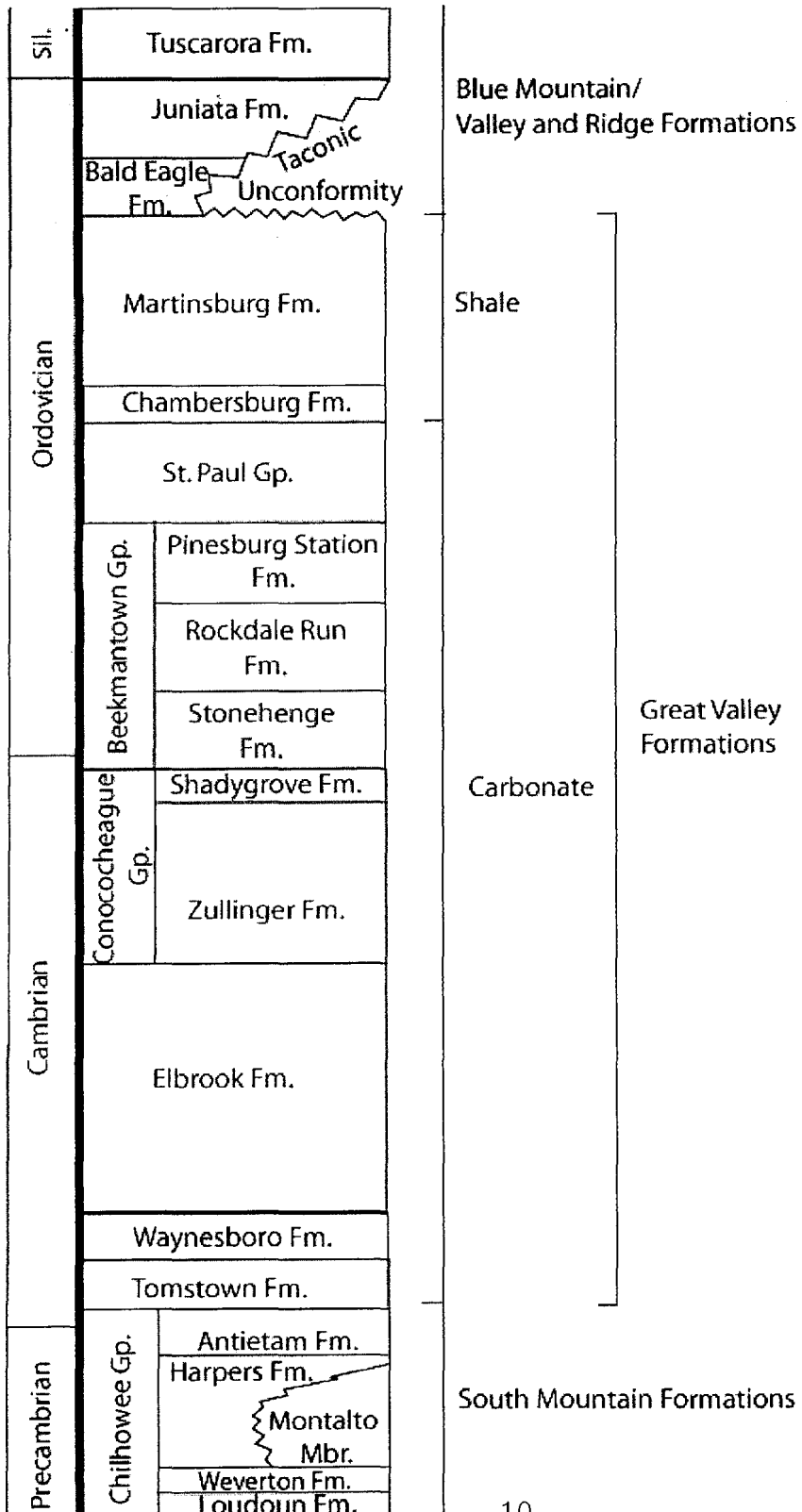


Figure 4. A stratigraphic column showing the geologic formations found in the Great Valley and flanking the Great Valley. South Mountain, Blue Mountain and Great Valley formations are grouped (Schultz, 1999).

from these ridges have deposited alluvial fans, terraces, and pediment alluvium unconformably atop the shale and carbonate of the Great Valley.

The contrasting shale-carbonate rock types in the Great Valley are mirrored by contrasting erosion processes. The shale outcrop belt is eroded primarily by physical abrasion in river channels and hillslope creep in the interfluvies. The sediment (Sevon, 1989) and water discharge in the shale drainage basins is proportional to the planimetric area of the basin. Published rates of mechanical erosion for the non-glaciated portion of the Appalachians, including the Great Valley, range from about 10 to 30 m/my (Reuter, 2004; Sevon, 1989). In contrast, the carbonate outcrop belt is eroded primarily by dissolution resulting in large portions of the landscape being underdrained. Discharge in these carbonate basins does not scale proportionally to drainage area (Potter, 2001), indicating a mismatch between topography, rates of surface processes, and the routing of water through this part of the landscape. Published rates of carbonate dissolution range from 17 m/m.y. (Potter, 2001) to ~30 m/m.y. (White, 1984; 2000). It is not known which, if any, of the strike parallel drainages (shale vs. carbonate) pace landscape change in the Great Valley, but the results of this study do shed some light on this specific question.

## **Base Level and Experimental Design**

Base level is a central concept in geomorphology that describes the level to which erosion of a landscape can proceed (Powell, 1875). Sea level is ultimate or final base level, but throughout a drainage basin, there are many local base levels typically defined by the mean elevation of a characteristic stream reach. The Great Valley is an ideal location to isolate the effects of local and ultimate base level by studying the evolution of the various asymmetric divides between the strike parallel drainages. Between eastern Pennsylvania and southern Virginia a series of five major strike parallel, transverse drainages, The Delaware, The Schuylkill, The Susquehanna, The Potomac, and the James Rivers from north to south respectively, cut through the Great Valley. Generally, there are two strike parallel drainages that are tributary to the transverse drainages. One tributary flows in the shale while the other flows in the carbonate. This drainage structure within the Great Valley creates a series of nested base levels (Powell, 1875): local, regional and ultimate. Substrate exerts the strongest influence on local base level within first and second order watersheds, which are concentrated on the dip parallel systems that feed into the major transverse drainages (Braun, 1983). The rates of dissolution in the carbonate drainages versus the rates of physical erosion control base level in these drainages. Other factors that can influence base level are insignificant within these small parallel drainages because their small area prevents differential influence from factors such as climate or tectonics. In the largest, ultimate, scale of base level, sea level, we can assume that any changes in sea level were experienced equally between the major transverse drainages.

It is the regional scale of base level for the Great Valley that may be the most telling about its evolution and is the most complicated. Regional base level is controlled by the major transverse drainages, which are strike parallel to the Great Valley. As the transverse drainages breached the Blue Ridge and extended into the Great Valley, they exposed their tributaries to a new, lower base level. If the Blue Ridge breaching varies from north to south, a general space for time substitution can be made. Instead of watching one part of the Great Valley evolve over time, the differential breaching of the Great Valley and Blue Ridge by the transverse drainages allows an examination of different stages of landscape evolution in different places at the same time. This differential expression of base level fall is expressed, for example, in the different incision rates of the Susquehanna and Potomac Rivers, at approximately 10-20 m/m.y. (Reusser, 2004), versus the James River, at between 160 m/my (Harbor, 2000) and 110 m/my (Ries, 1998). These differential incision rates indicate that translation of base level fall upstream, for example, is a more recent event for the James River and its tributaries than it is for the Susquehanna River (Hancock, 2004) and its tributaries. This north to south sequential breaching of the Blue Ridge makes the space for time substitution approach viable and it is an important prerequisite to the experimental design.

Divides between the major transverse rivers are characteristically low in relief. It is the low order streams flanking these divides that would be the most sensitive to changes in base level (Merritts and Vincent, 1989) and determine whether the divides are fixed features or dynamic components of the Great Valley landscape. Assuming comparable discharges of first order streams, those with higher slopes will have higher stream power values (Bagnold 1973, 1975) and will thus be able to do more physical

erosion (Gilbert, 1877). If streams on one side of the divide have systematically higher gradients, that side of the divide will capture opposing drainage, through headward migration causing an overall migration of the divide. It is important to point out that this divide migration process only strictly applies for the shale bedrock portion of the Great Valley as the limestone bedrock portion is characterized by chemical (dissolution) rather than physical erosion.

An experiment is designed to unravel the landscape evolution of the major drainage divides in the Great Valley with the intent of this history having some bearing on the applicability of the major paradigms for Appalachian landscape evolution. The experiment consists of two major methodological components; large scale extraction of basin and channel metrics using digital elevation model (DEM) and a small field study in the Cumberland Valley which is between the Susquehanna River to the north and east and the Potomac River to the south and west. Metrics extracted from the DEM include two whole basin metrics: drainage density and hypsometry. Data for longitudinal (long) profile modeling was also extracted from the DEM but was restricted to the first order streams flanking the transverse drainage divides. The field study sought to characterize the extent, composition, and texture of known upland gravel deposits in the Cumberland Valley. Merging these two data sets allows for the interpretation of large amounts of data across the regional scale of the Great Valley while concentrating on one divide in which to find surficial evidence of fixed or migrating divides.

### *DEM analyses*

Digital elevation models (DEMs) were acquired from the USGS seamless server and other commercial internet services such as Mapmart. Both 10m and 30m resolution DEMs were used for this study. The 30m data was used only in those areas for which 10m data were not available. Sensitivity analyses were conducted on watershed topography constructed from 30m and 10m resolution DEM data in order to assess how DEM resolution affected the values of metrics extracted from the DEM.

All DEM-based analyses were conducted in a Geographic Information Systems (GIS) using the software ArcGIS version 8.3. Whole-basin metrics extracted from the DEM included hypsometry and drainage density. Hypsometry (Strahler, 1952) relates the area of the basin at any one elevation to the mean elevation of the total basin. It is controlled by rock type, basin size and aggradation or erosion of a basin. Hypsometric interval values allow the comparison of drainage efficacy between basins. It is reasonable to assume that younger landscapes will have a larger area at higher elevations, therefore basins with hypsometric curves that show more area at higher elevations have had less time to remove the material and form efficient drainage networks.

Drainage density (eq. 1), in contrast, is the length of stream

$$Dd = \sum L / A \quad (\text{eq. 1})$$

Where  $Dd$  equals drainage density,  $L$  equals length and  $A$  equals area.

$$\frac{\text{stream\_length\_m}}{((\text{flow\_accumulation\_1\_} + \text{flow\_accumulation\_2\_}) * \text{cell\_spacing\_m}^2)} = \text{drainage\_density\_m}^{-1} \quad (\text{eq. 2})$$

channel in a basin divided by the area of the basin ( $m^{-1}$ ). Drainage density is dependent on hydrology, particularly infiltration rate, which is in turn dependent on climate and lithology, uplift and gradient (Glock, 1931).

Long profile modeling is useful as a technique to quantify the rates of rock uplift and fluvial erosion in tectonically active areas (Snyder, 2000; Duvall, 2004; Molin et al., 2004; Merritts, 1989). It has been applied to a much lesser degree in tectonically quiescent areas (Zaprowski et al., 2005) such as this and all of the details regarding the relative influences of rock-type and climate have yet to be fully realized (Roe et al., 2002; Duvall et al., 2004). Nevertheless, most bedrock eroding rivers have concave up longitudinal profiles. In bedrock channels this is a result of detachment limited erosion processes while in alluvial channels it is the results of downstream grain size fining, an increase in discharge and an increase in channel width. Discharge ( $Q$ ) scales proportionally to drainage area ( $A$ ) and it has been found that the concave-up shape of long profiles tend to approximate a power function linked to drainage area such that channel slope ( $S$ ) is equal to drainage area raised to a power:

$$S = k_s A^\theta, \quad (\text{eq. 3}).$$

Empirical data worldwide indicates that  $\theta$ , termed the profile concavity, ranges from about 0.2 to 1.0 with a mode of about 0.4 or 0.5. The overall profile steepness is  $k_s$  and it has a wide range of values depending on the units of area chosen for the analysis.

The utility of equation 3 is realized when the concavity and steepness of a river long profile can be related to the rate of incision and long term erosion of the landscape. The erosion rate ( $E$ ) of predominantly detachment limited, perennial channels is generally modeled as proportional to a power law function of basal shear stress.



$$E = KA^m S^n, \quad (\text{eq. 4})$$

Equation 3 assumes steady uniform flow, conservation of water in the channel, a linear relationship between discharge and upstream drainage area and channel width that increases as a function of the square root of the discharge. The exponents  $m$  and  $n$  are real, positive numbers that are determined by channel erosion processes and  $K$  is a constant that adjusts for rock type and climate. Assuming the channel is at equilibrium, which requires that the change in channel elevation over time ( $dz/dt$ ) is zero and that channel erosion ( $E$ ) is equal to rock uplift ( $U$ ),

$$dz/dt = 0 = U - E = U - KA^m S^n \quad (\text{eq. 5})$$

Equation (4) can be rearranged to isolate channel slope as a function of drainage basin area,

$$S = (U/K)^{1/n} A^{-m/n} \quad (\text{eq. 6})$$

Equation 5 has a similar form as equation 2 and allows for direct comparison between profile steepness ( $k_s$ ) and  $(U/K)^{1/n}$  and between  $\theta$  and  $m/n$ . The same linear relationship (in log space) between  $\log A$  and  $\log S$  in both equation 1 and 4 allow for direct comparison between actual and modeled channel concavities and steepnesses (fig. 5). When modeling steepness it is important to have a constant  $\theta$ ; the actual value of  $\theta$  is unimportant and many studies have used 0.4 or 0.5 (Duvall et al., 2004).

The idea that is pursued in this study is that the degree of long profile equilibrium (or disequilibrium) should be reflected in the concavity and steepness values of channels in the drainage divide areas of the Great Valley. Comparing steepness values, for example, for the first order streams in the divide regions of the major transverse drainages should allow us to determine if these channels are well adjusted to base level

and if either side of each divide has a competitive advantage, leading to drainage capture and divide migration.

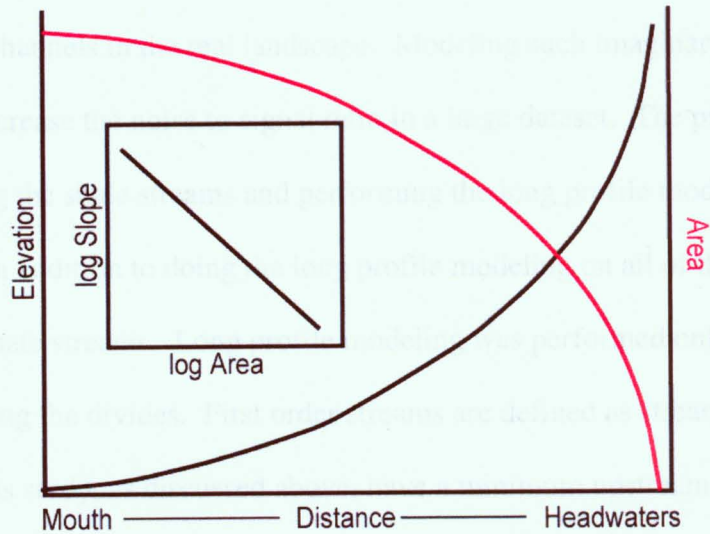


Figure 5. A theoretical graph showing the relationship between elevation along a long profile and upstream drainage area along the same long profile. When the upstream drainage area and the slope are converted to a logarithmic scale, a linear relationship becomes apparent.

The parallel bands of shale and carbonate bedrock introduce an interesting wrinkle to the long profile modeling approach. The method requires that a minimum threshold be determined which defines the smallest amount of upstream drainage area needed to create a stream. On the shale, field observations show that a good value for minimum upstream drainage area is  $\sim 0.5\text{km}^2$ . In contrast, the carbonate bedrock drainage is difficult, if not impossible to characterize as it has disappearing streams, springs, and underdrained reaches. Thus, due to the fact that much of the water flows

through underground karst systems, the assumption that an excess of  $0.5\text{km}^2$  upstream drainage area will yield a channel is false and using any fixed single value for upstream drainage area in the carbonate system will yield erroneous stream channels in a DEM where there are no channels in the real landscape. Modeling such imaginary stream channels tends to increase the noise to signal ratio in a large dataset. The problem is resolved by isolating the shale streams and performing the long profile modeling on this sub-set of the data in addition to doing the long profile modeling on all of the data, including the carbonate streams. Long profile modeling was performed only on the first order streams flanking the divides. First order streams are defined as streams with no tributaries and in this study, as discussed above, have a minimum upstream drainage area of  $0.5\text{km}^2$ . Second order streams begin at the junction of two first order streams. This junction is where the first order streams were truncated for modeling purposes. Only first order streams are used for modeling because they are the most sensitive to base level changes. Two results are produced: (1) a subset of streams on the shale bedrock that quantifies the steepness of opposing flanks of a transverse river drainage divide, (2) an assessment of the noise to signal ratio (fig. 6).

Long profile modeling requires significant processing of topographic data to reduce the noise to signal ratio that results from the coarseness of the DEM data and the various flow routing routines in a GIS that are restricted to determining gradients on only an eight vector rectilinear grid. Initially, much of the noise in the data was eliminated by choosing to examine values for only the first order. First order streams, streams with no tributaries, were isolated using the streamorder command in ArcGIS. These low order streams are more sensitive to changes in base level. Data processing is accomplished by

Figure 6. The flow accumulation map (DEM) used to find a subset of concavity

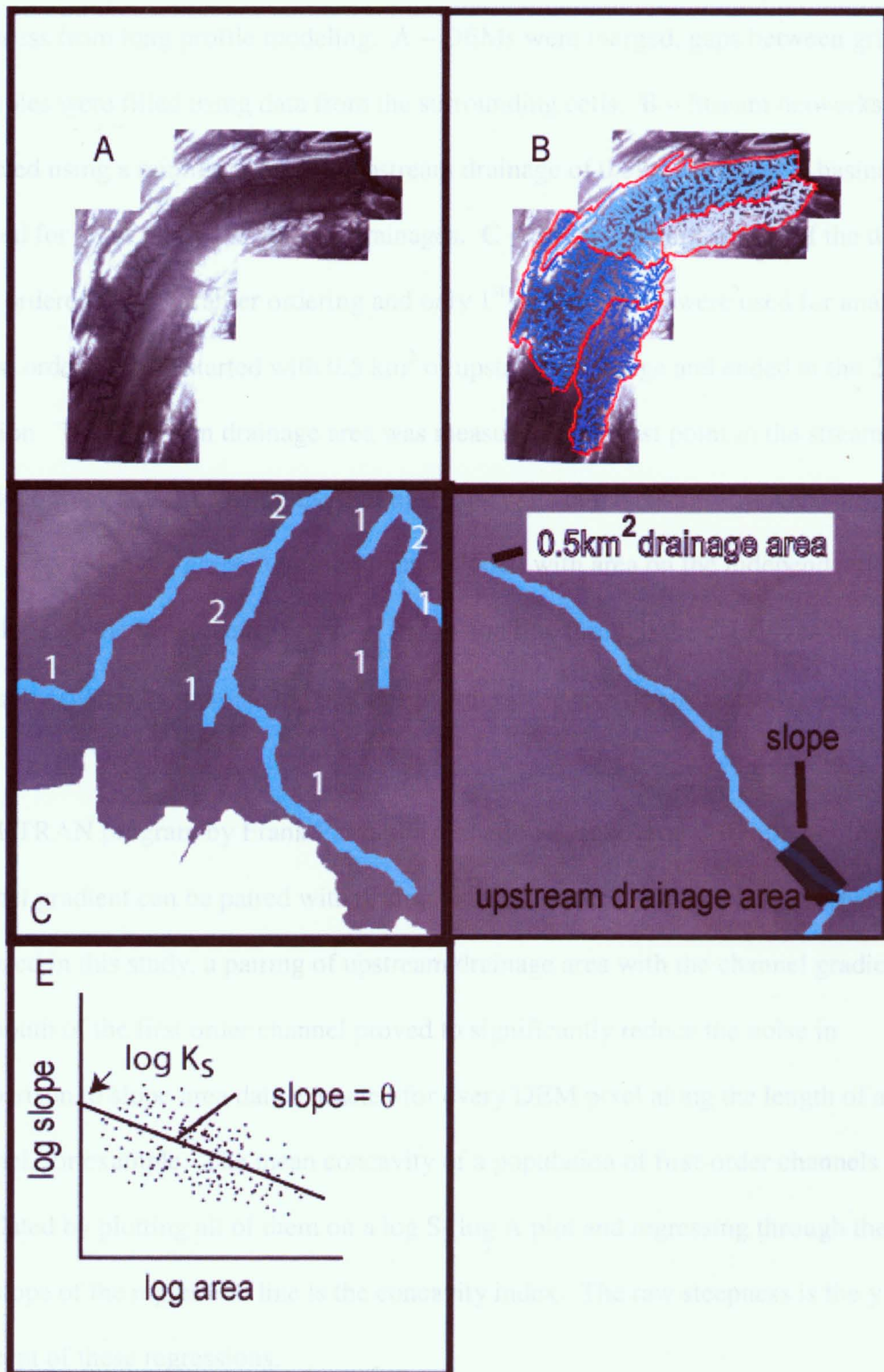


Figure 6. The steps taken to use raw DEM data to extract values of concavity and steepness from long profile modeling. **A** – DEMs were merged, gaps between grids and any holes were filled using data from the surrounding cells. **B** – Stream networks were modeled using a minimum area of upstream drainage of  $0.5\text{km}^2$ . Drainage basins were defined for all of the strike parallel drainages. **C** – Streams on either side of the divide were ordered using Strahler ordering and only 1<sup>st</sup> order streams were used for analysis. **D** – First order streams started with  $0.5\text{ km}^2$  of upstream drainage and ended at the 2<sup>nd</sup> order junction. The upstream drainage area was measured at the last point in the stream while the slope was calculated using the # of upstream cells in the basin. **E** – Area-Slope data were exported into a graphing program and plotted with area on the independent(x) axis and slope on the dependent(y) axis. A regression line through the data gives the negative concavity ( $-\theta$ ) as the inverse log of slope and the steepness ( $k_s$ ) as the y-intercept.

a FORTRAN program by Frank Pazzaglia that allows for several different options of how channel gradient can be paired with upstream drainage area. For the first order streams analyzed in this study, a pairing of upstream drainage area with the channel gradient at the mouth of the first order channel proved to significantly reduce the noise in comparison to slope-area data extracted for every DEM pixel along the length of a channel, for example. The mean concavity of a population of first-order channels is calculated by plotting all of them on a log S- log A plot and regressing through the data. The slope of the regression line is the concavity index. The raw steepness is the y-intercept of these regressions.

In order to model steepness, a concavity index of 0.5 was chosen. Being able to directly compare modeled steepness and concavity for the basins on either side of the divides separating the rivers flowing transverse to the Great Valley should quantify which divide flanks are steeper and more in equilibrium with the prevailing base level conditions.

### *Field analyses*

Field data were collected in the Cumberland Valley of south-central Pennsylvania. The divide between the Susquehanna and Potomac Rivers cuts orthogonally across the center of the Cumberland Valley. Similarly to the other divides between the transverse rivers of the Great Valley, it has low relief and the uplands are locally mantled with gravel deposits. The distribution and composition of upland gravels in the divide between the Potomac and Susquehanna Rivers in the Great Valley would support divide migration rather than divide stability as argued by Davis. Conversely, Hack used upland gravels in the Potomac Basin to support topographic inversion and dynamic equilibrium. The objective of the field study is to characterize the spatial extent, texture and composition of these deposits. The soil surveys of Cumberland and Franklin Counties, PA (Long, 1975; Zarichansky, 1986) were used to help determine the extent of fluvial deposits, characteristically rounded cobbles, in the divide area. Soil descriptions, which contain adjectives such as gravelly or cobbly, served as a good starting point when looking for cobble deposits. The location of cobble deposits was noted using a GPS unit. A map of the surficial deposits was made using the field data collected on digital copies of the USGS 7.5' topographic maps.

The texture and composition of deposits were characterized by sampling each deposit. A sample of cobbles was collected from each deposit by randomly placing a 1 m<sup>2</sup> box made of 1/4" PVC pipe on the ground and collecting all of the cobbles that fell within the box. This was repeated until enough cobbles were collected for a representative sample from each location. The A, B and C axis of each cobble was measured. A is the longest axis of the rock, while C is the shortest and B is the intermediate axis with all axes being perpendicular to each other. These data allow for the quantification of the shape of each cobble and the average shape of cobbles for each deposit. Using the assumption that form follows process, cobbles with different proportions were shaped by different processes. Average cobble shape for each deposit should be representative of the major process, which emplaced the deposit. Then each cobble was broken apart and the rock type, internal color, and weathering rind, if any, were measured. Rind thickness is highly variable in some cobbles and uniform in others. In cases, where the rind thickness was variable an average thickness was taken using the thickest and thinnest rind sections within the cobble. Weathering rinds in cobbles are caused by movement and leaching of elements from the outer edge. They are indicative of weathering. If rock type, climate and hydrology remain constant between deposits weathering rinds may be used to differentiate deposit age. Thin sections were made of representative samples from each site to look for textural evidence of compositional differences.

## Results

### *Field-based observations*

Field data include observations centered on the map distribution, weathering, and textural characteristics of upland gravels deposits in a part of the Cumberland Valley spanning the divide between the Susquehanna and Potomac rivers. An upland gravel is defined as a deposit of well rounded, and typically hard pebble, cobble, and rare boulder-size clasts, mixed with sand and soil, typically found on low-relief interfluves. Upland gravels are rarely, if ever, stratified but rather occur as a thin mantle or surface lag. Density of clasts varies from deposit to deposit, but the fact that mapping of these deposits is best accomplished in the late spring and early summer when agricultural fields have been plowed speaks to the general sparseness of these deposits in the landscape.

Five main upland gravel deposits have been mapped (see map plate 1 and fig. 7). These sites are all in cultivated fields and were identified in the spring, after the fields were tilled but before extensive crop growth. Gravel occurrence in these sites ranges from dense, 42 cobbles/m<sup>2</sup> at the Salem deposit, to very sparse, 2.75 cobbles/m<sup>2</sup> at the Roxbury Rd. deposit. At sites with high densities of cobbles on the surface, cobbles were also found at depths of 1m or more below the surface. Upland gravel deposits are closely correlated with a specific soil, the Weikert shaly silt loam (Long, 1975), identified on the Franklin County Soil Survey is typically associated with well-drained interfluves. In this way, soil survey maps are a useful guide to locating upland gravels in this area.

In contrast to the upland gravel deposits, thick deposits of alluvial fan sand and gravel occur along the southeast flank of the Cumberland Valley, typically at the mouth of steep drainages flowing west out of South Mountain. The sand and gravel quarry



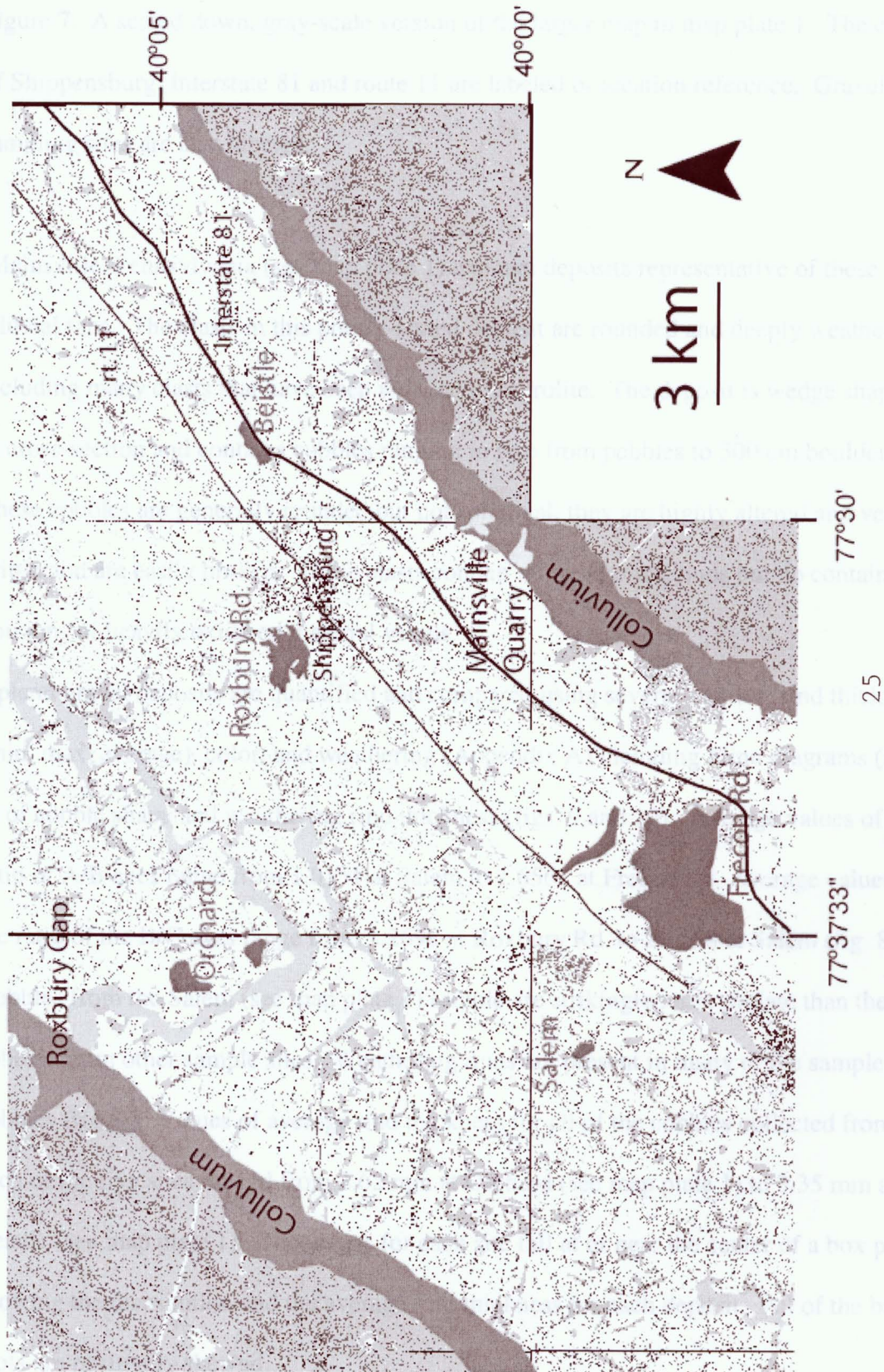


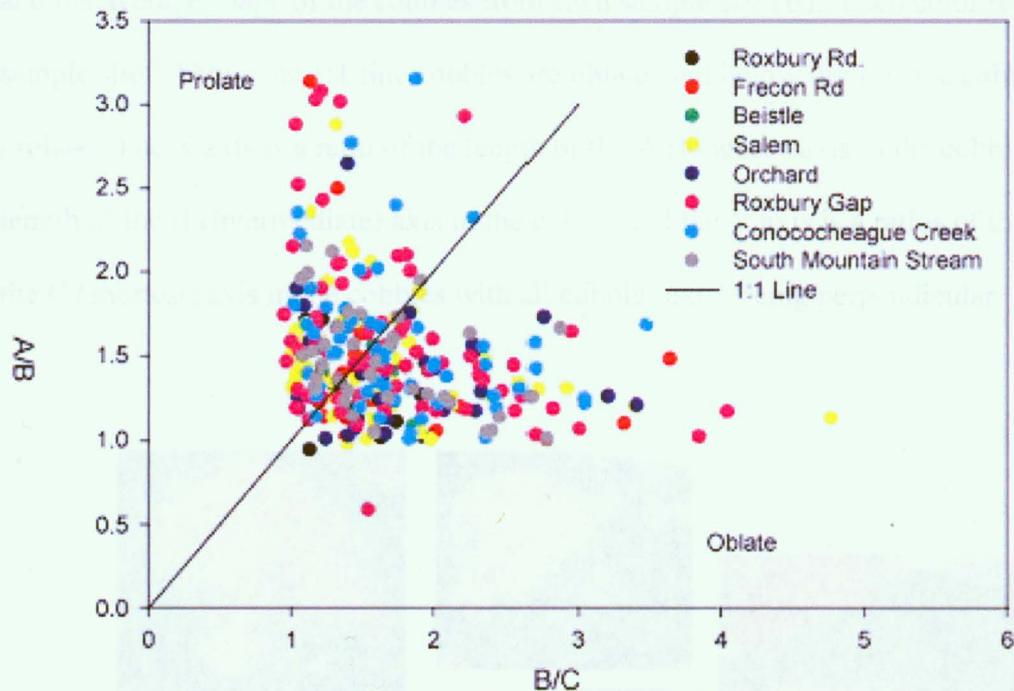
Figure 7. A scaled down, gray-scale version of the larger map in map plate 1. The city of Shippensburg, Interstate 81 and route 11 are labeled or location reference. Gravel sampling sites are also labeled.

Mainsville, Pennsylvania (see map plate 1) exposes deposits representative of these alluvial fans. The clasts in this poorly-sorted deposit are rounded and deeply weathered, including many clasts that have been reduced to saprolite. The deposit is wedge shaped in cross-section and contains cobbles ranging in size from pebbles to 300 cm boulders. These cobbles are generally rounded but not spherical; they are highly altered and very brittle and are easily broken. These clasts contain no weathering rinds but do contain horizons of heavily oxidized material versus.

Upland gravel deposits are quantified and compared using several metrics; rind thickness (min, max, average), color, and weathering (Appendix A) including Flinn diagrams (fig. 8) of cobble shape and weathering rind thickness (figs. 9 and 10). Average values of the ratio of A/B axes range from 1.0151 at Salem to 1.6562 at Frecon Rd. Average values of the ratio of the B/C axes range from 1.2698 at Roxbury Rd. to 2.1598 at Salem (fig. 8). Cobbles from the Salem (see map plate 1) sample are strikingly more prolate than the cobbles from other sample sites. Weathering rinds are present in many of the sample cobbles (fig. 9). Values of average rind thickness for all of the cobbles collected from each of the five sites ranged from 2.62 mm at Orchard (see map plate 1) to 3.35 mm at Beistle (see map plate 1). The means for each site fall at or near the center of a box plot showing the distribution and the average rind thickness for each deposit. All of the box plots are positively skewed.

**A**

Flinn Diagram of Cobble Shape

**B**

Flinn Diagram of Average Cobble Shape

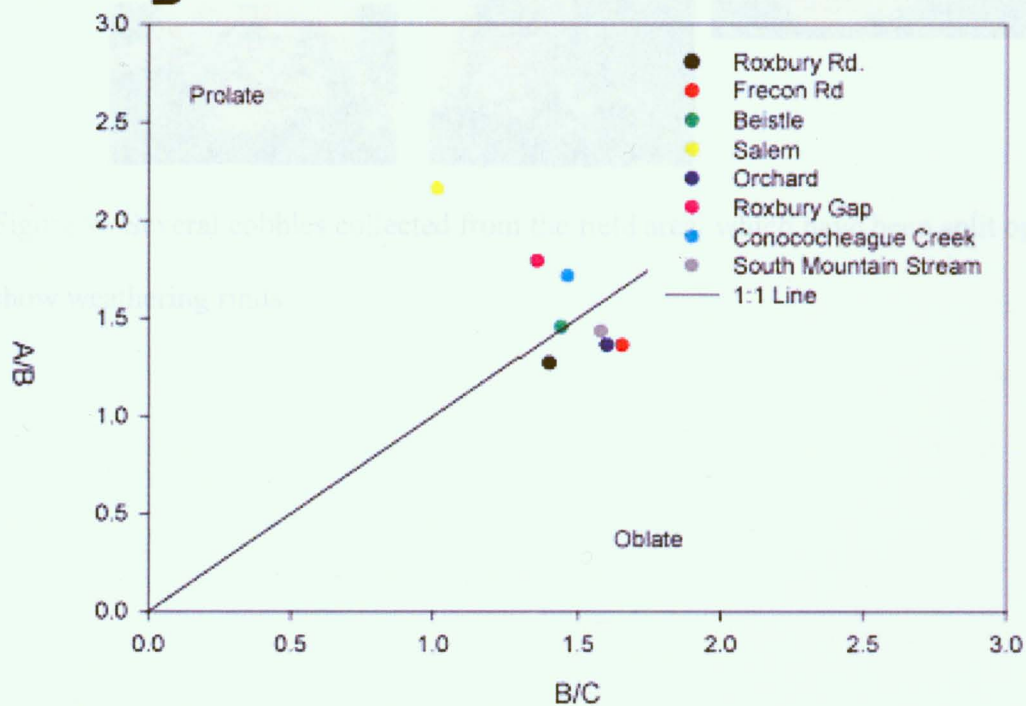


Figure 8. Flinn diagrams showing the shape of all the cobbles from each sample site (A) and the average shape of the cobbles from each sample site (B). Each color represents one sample site. Above the 1:1 line cobbles are oblate and below the 1:1 line cobbles are prolate. The X axis is a ratio of the length of the A (longest) axis in the cobble to the length of the B (intermediate) axis in the cobble and the Y axis is a ratio of the B axis to the C (shortest) axis in the cobbles with all cobbles axis' being perpendicular.

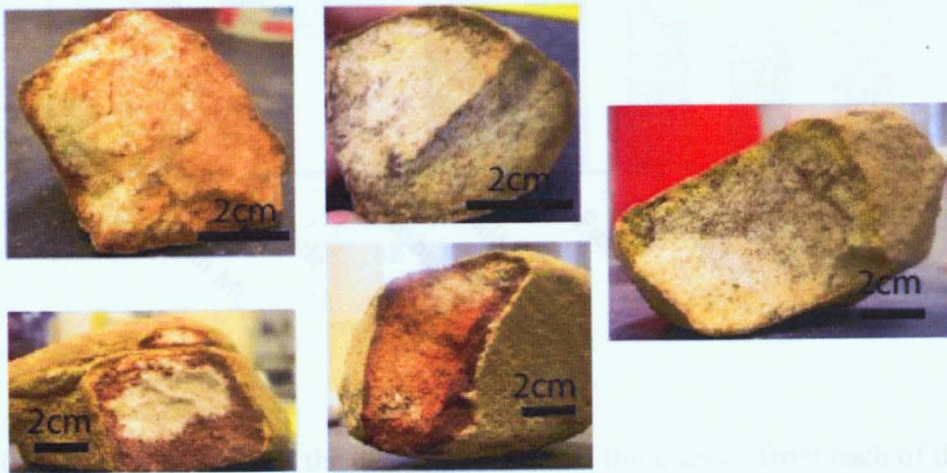


Figure 9. Several cobbles collected from the field area, which have been split open to show weathering rinds.

## Rind Thickness Variation

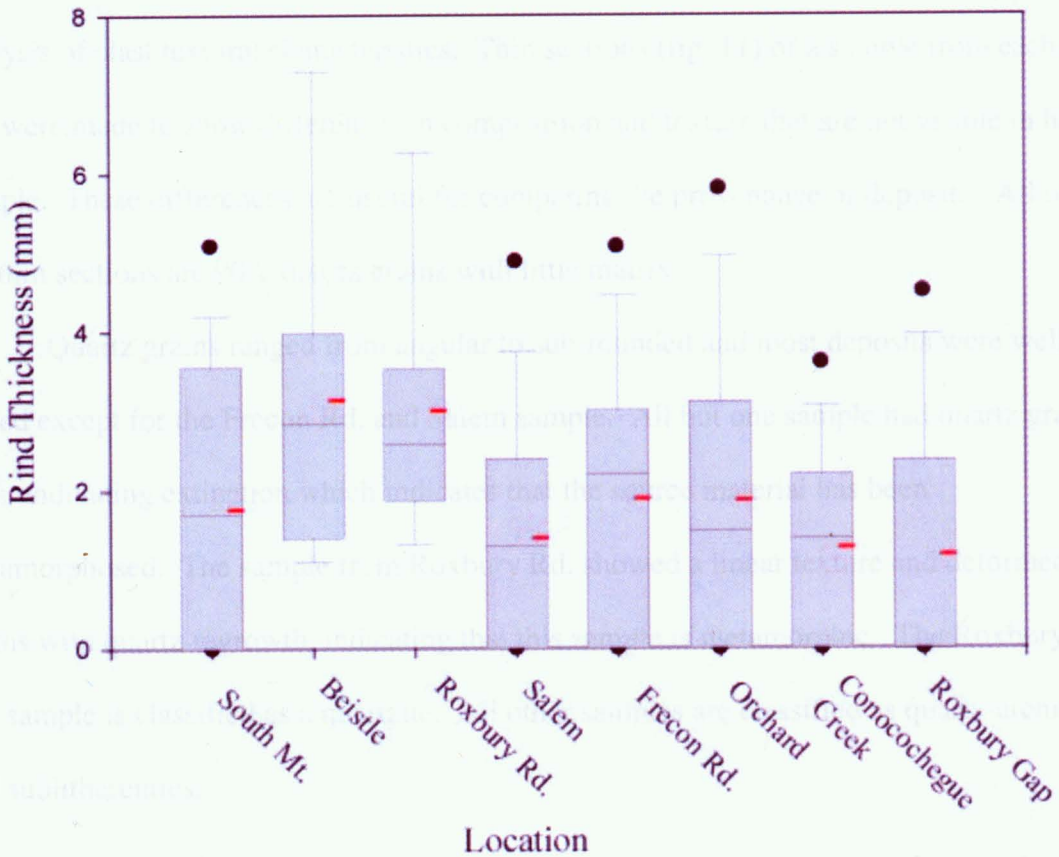
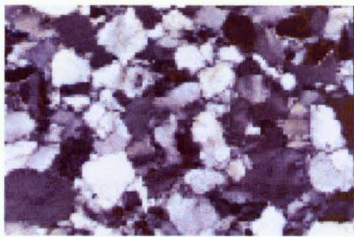


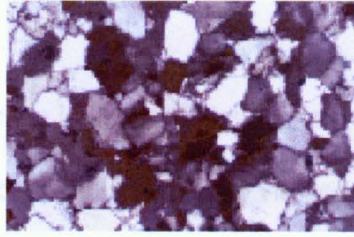
Figure 10. A box plot showing the distribution of rind thicknesses from each of the sample site. The black dots indicate the 5<sup>th</sup> and 95<sup>th</sup> percentile outliers, the solid black line is the median of rind thicknesses while the red dash on the right side of each box is the mean rind thickness. The sample sites are organized with the southernmost sample site on the left and the northernmost on the left. South Mt., Roxbury Gap and Conococheague Creek are modern streams.

Upland gravel characterization is rounded out through the use of thin section analysis of clast textural characteristics. Thin sections (fig. 11) of a sample from each site were made to show differences in composition and texture that are not visible in hand sample. These differences are useful for comparing the provenance of deposits. All of the thin sections are 90% quartz grains with little matrix.

Quartz grains ranged from angular to sub-rounded and most deposits were well sorted except for the Frecon Rd. and Salem sample. All but one sample had quartz grains with undulating extinction which indicates that the source material has been metamorphosed. The sample from Roxbury Rd. showed a linear texture and deformed grains with quartz regrowth, indicating that this sample is metamorphic. The Roxbury Rd. sample is classified as a quartzite. All other samples are classified as quartz-arenites and sublitharenites.



**A. Orchard**



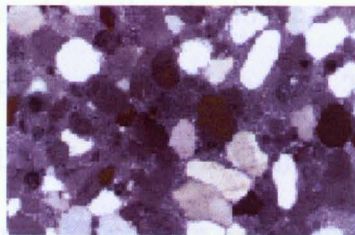
**B. Beistle**



**C. Roxbury Rd.**



**D. Frecon**



**E. Beistle**



**F. Roxbury Rd.**



**G. Salem**



**H. Salem**

2mm



Figure 11. Thin section photographs of cobbles from each of the sampling sites. All of the cobbles are mainly composed of quartz. The thin sections from Beistle has more matrix than the other cobbles and one of the thin sections from the Roxbury Rd. (C) sample shows quartz regrowth and linear texture.

### *Map-based Metrics*

The Great Valley landscape is quantified using map and digital topography based measurements of specific metrics that are typically viewed as carrying information related to time-dependent landscape evolution. Specifically, drainage density and hypsometry values were calculated for all basins in the study area. These larger scale metrics allow for quantified comparison between basins. The drainage densities (table 1) for the northern six drainages; Lehigh west, Schuylkill east, Schuylkill west, Susquehanna east, Susquehanna west, and Potomac north are  $\sim 0.001\text{m}^{-1}$  (between 0.000999 and 0.00155). The southernmost drainage, which flows south into the James River, has a thin sections from the Roxbury Rd. sample shows quartz regrowth and linear texture. drainage density value of  $0.000279\text{m}^{-1}$ ; this is the lowest drainage density value in the study. The highest drainage density value in the study,  $0.00364\text{m}^{-1}$ , is in the Potomac south drainage, the second southern-most drainage. A sensitivity study designed to test the effect of different resolution DEM on the measuring of a landscape metric like drainage density was conducted for the Lehigh west drainage basin. The test resulted in a drainage density value of  $0.0105\text{m}^{-1}$  for both 10- and 30-meter DEM. Thus, the sensitivity is low enough that different DEM resolutions probably do not significantly skew the results.



Table 1. Drainage density values for the Great Valley

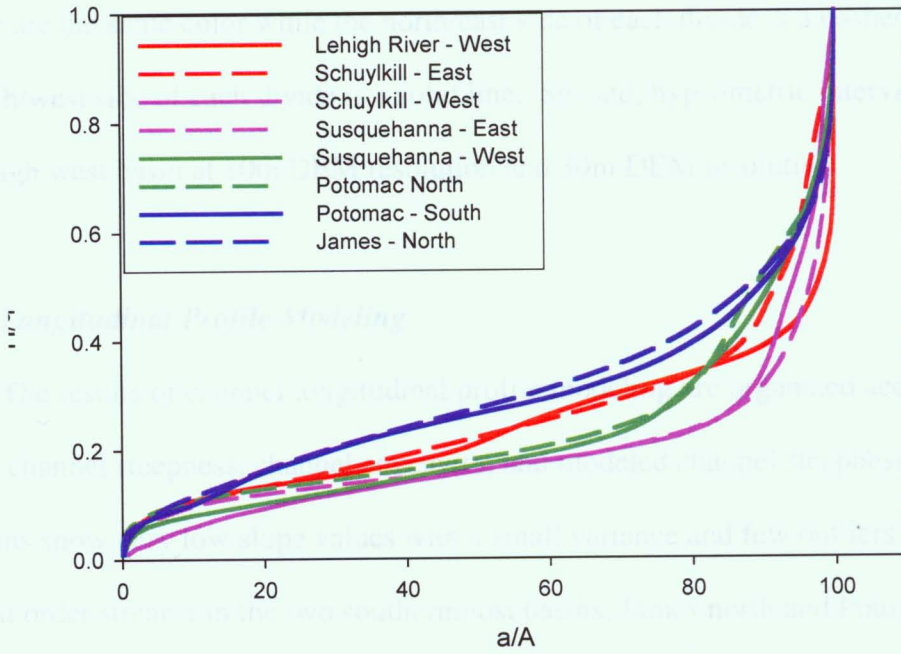
Basin	Stream Length(m)	Basin Area (cells)	Cell Size (m <sup>2</sup> )	Drainage Density (m <sup>-1</sup> )
Lehigh west (10m)	489401.3308	4676097	10m	0.00105
Lehigh west (30m)	512100.2	543066	30m	0.00105
Schuylkill east	404075.6938	4045090	10m	0.000999
Schuylkill west	589279.6676	5663872	10m	0.00104
Susquehanna east	1076036.125	10721021	10m	0.00100
Susquehanna north	1970965.283	18567350	10m	0.00106
Potomac north	2219724.269	14367315	10m	0.00155
Potomac south	9366757.2922	2858886	30m	0.00364
James north	2617303.92	10439009	30m	0.000279

Hypsometric curves and values quantify the distribution of elevation in a basin. The curves for each basin are more similar in both shape and values to the basin with which they share a divide than any other basin. Hypsometric curves (fig. 12) and mean hypsometric values (table 2) were found to be similar for the 10m and 30m data in the Lehigh west basin. The southernmost basin, James north, has most of its basin area at higher elevations. Elevations of basin areas decrease northward until the Schuylkill west and Lehigh basin, which do not follow a general lowering trend. These basins were the terminus of glaciation during the last glacial maximum.

Table 2. Mean Hypsometric Values

Basin	Mean Hypsometric Values
Lehigh west	97.5229
Schuylkill east	91.9952
Schuylkill west	94.0681
Susquehanna east	96.5011
Susquehanna west	90.9955
Potomac north	89.0213
Potomac south	89.8670
James north	88.1799

## HYPSONOMETRIC INTERVAL CURVES



### Lehigh Basin Sensitivity for Hypsometric Intervals

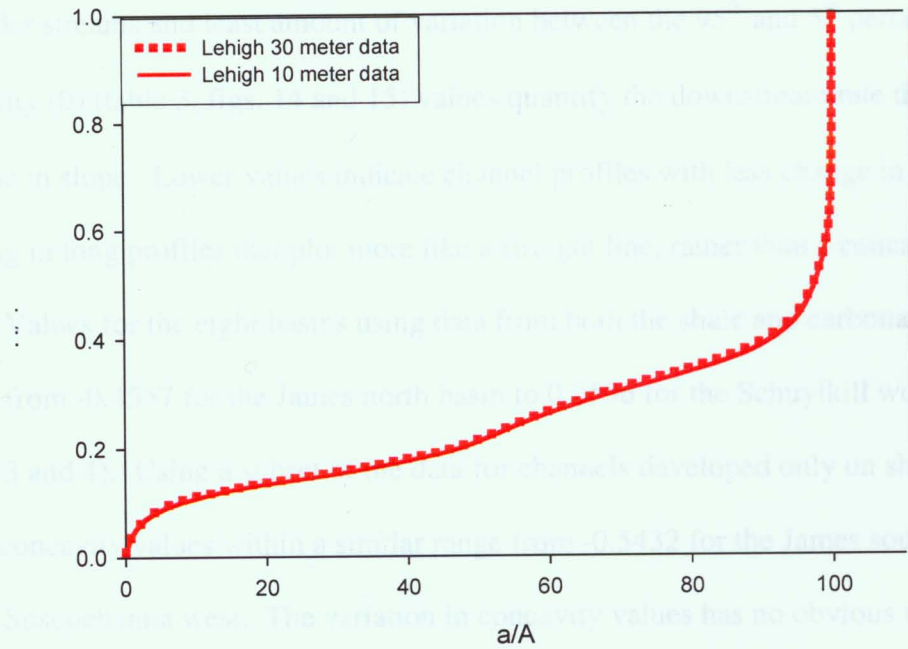


Figure 12. First, hypsometric plots for each of the eight basins studied. Basins that share a divide are the same color while the north/east side of each divide is a dashed line and the south/west side of each divide is a solid line. Second, hypsometric interval curves for the Lehigh west basin at 10m DEM resolution and 30m DEM resolution.

### *Longitudinal Profile Modeling*

The results of channel longitudinal profile modeling are organized according to the raw channel steepness, channel concavity, and modeled channel steepness. Most of the basins show very low slope values with a small variance and few outliers (fig 13). The first order streams in the two southernmost basins, James north and Potomac south, show higher slope values, more variation, and more outliers. Additionally, the northern side of the Cumberland Valley (Susquehanna west) shows the lowest average slope for first order streams and least amount of variation between the 95<sup>th</sup> and 5<sup>th</sup> percentile. Concavity ( $\theta$ ) (table 3, figs. 14 and 15) values quantify the downstream rate that channels decrease in slope. Lower values indicate channel profiles with less change in slope, resulting in long profiles that plot more like a straight line, rather than a concave-up curve. Values for the eight basins using data from both the shale and carbonate streams ranged from -0.4557 for the James north basin to 0.2536 for the Schuylkill west basin (tables 3 and 4). Using a subset of the data for channels developed only on shale bedrock shows concavity values within a similar range from -0.5432 for the James south to 0.2535 for the Susquehanna west. The variation in concavity values has no obvious trend for each set of data.

## Distribution of Slope Values

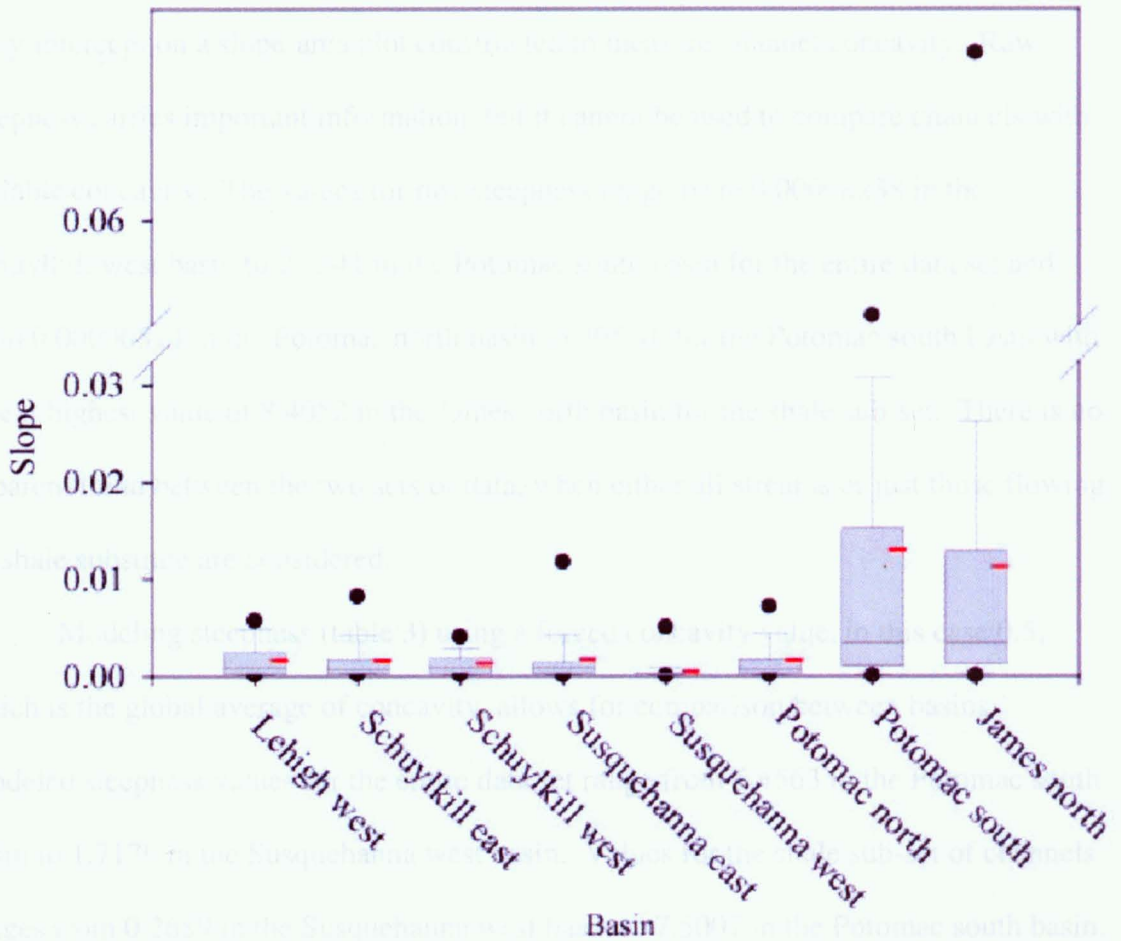


Figure 13. A box plot of slope variation for the study basins. Black dots show the 5<sup>th</sup> and 95<sup>th</sup> percentile values. The red dash shows the mean slope value, while the black line within the box is the median slope value. The gray box encompasses the 25<sup>th</sup> or 75<sup>th</sup> percentile of slope values. The break in scale on the y axis only affects the Potomac south and James north basins.

Raw channel steepness (table 3, figs. 14, and 15) is a sister metric represented as the y-intercept on a slope-area plot constructed to measure channel concavity. Raw steepness carries important information, but it cannot be used to compare channels with variable concavity. The values for raw steepness range from 0.00008238 in the Schuylkill west basin to 2.3541 in the Potomac south basin for the entire data set and from 0.00006514 in the Potomac north basin to 305.46 for the Potomac south basin with a next highest value of 8.4052 in the James north basin for the shale sub-set. There is no apparent trend between the two sets of data, when either all streams or just those flowing on shale substrate are considered.

Modeling steepness (table 3) using a forced concavity value, in this case 0.5, which is the global average of concavity, allows for comparison between basins. Modeled steepness values for the entire data set range from 5.4563 in the Potomac south basin to 1.7179 in the Susquehanna west basin. Values for the shale sub-set of channels ranges from 0.2689 in the Susquehanna west basin to 7.5007 in the Potomac south basin. Variations in modeled steepness values are similar with the entire data set and the shale sub-set. Both sets of data have their lowest values in the Susquehanna west basin and modeled steepness values increase in the two basins to the east/north and the two basins to the south/west (fig 2).

The values of concavity, raw steepness and modeled steepness for the Lehigh west basin vary as a function of DEM resolution (table 4). Raw steepness values are  $4.011 * 10^{-3}$  and  $1.488 * 10^{-3}$  for Lehigh west 30m and 10m data, respectively. Concavity values are -0.04543 and 0.05764 for Lehigh west 30m and 10m data, respectively. Modeled steepness values are  $4.009 * 10^{-3}$  and 3.2382 for Lehigh west 30m and 10m

data, respectively. Unfortunately, the 10m resolution data set is not complete for any of the study area, particularly, the divide between the James and Potomac Rivers. Data with a resolution of 30m<sup>2</sup> was used instead for the entire basins north of the James and south of the Potomac. Internally, comparison between concavity, raw and modeled steepness can be made because these data have the same resolution.

Table 3. Longitudinal profile modeling values

All Streams		Shale Streams	
<b>Lehigh west</b>		<b>Lehigh west</b>	
raw steepness (log)	-2.8272	raw steepness (log)	-3.6440
raw steepness	1.488e-3	raw steepness	2.269e-4
concavity	0.05764	concavity	0.2064
r <sup>2</sup>	3.749e-4	r <sup>2</sup>	5.711e-3
modeled steepness (log)	0.5103	modeled steepness (log)	0.5996
modeled steepness	3.2382	modeled steepness	3.9774
<b>Schuylkill east</b>		<b>Schuylkill east</b>	
raw steepness (log)	0.02704	raw steepness (log)	0.6367
raw steepness	1.0642	raw steepness	4.3316
concavity	-0.4272	concavity	0.5234
r <sup>2</sup>	0.01971	r <sup>2</sup>	0.02868
modeled steepness (log)	0.4765	modeled steepness (log)	0.4975
modeled steepness	2.9957	modeled steepness	3.1441
<b>Schuylkill west</b>		<b>Schuylkill west</b>	
raw steepness (log)	-4.0842	raw steepness (log)	-2.9234
raw steepness	8.238e-5	raw steepness	1.193e-3
concavity	0.2536	concavity	0.09651
r <sup>2</sup>	7.739e-3	r <sup>2</sup>	9.073e-4
modeled steepness (log)	0.4275	modeled steepness (log)	0.6673
modeled steepness	2.6761	modeled steepness	4.6484
<b>Susquehanna east</b>		<b>Susquehanna east</b>	
raw steepness (log)	-2.3050	raw steepness (log)	-2.6874
raw steepness	4.955e-3	raw steepness	2.054e-3
concavity	-0.06122	concavity	0.01251
r <sup>2</sup>	4.729e-4	r <sup>2</sup>	2.329e-5
modeled steepness (log)	0.2929	modeled steepness (log)	0.3564
modeled steepness	1.9629	modeled steepness	2.2720

<b>Susquehanna west</b>		<b>Susquehanna west</b>	
raw steepness (log)	-0.2868	raw steepness (log)	-2.8617
raw steepness	0.5166	raw steepness	1.3750e-3
concavity	-0.4129	concavity	0.02678
r <sup>2</sup>	0.03698	r <sup>2</sup>	4.076e-3
modeled steepness (log)	0.2350	modeled steepness (log)	-0.5704
modeled steepness	1.7179	modeled steepness	0.2689
<b>Potomac north</b>		<b>Potomac north</b>	
raw steepness (log)	-4.1605	raw steepness (log)	-4.1861
raw steepness	6.911e-5	raw steepness	6.514e-5
concavity	0.2482	concavity	0.2534
r <sup>2</sup>	7.901e-3	r <sup>2</sup>	6.669e-3
modeled steepness (log)	0.3279	modeled steepness (log)	0.2827
modeled steepness	2.1276	modeled steepness	1.9173
<b>Potomac south</b>		<b>Potomac south</b>	
raw steepness (log)	0.3718	raw steepness (log)	2.4849
raw steepness	2.3541	raw steepness	305.4063
concavity	-0.4387	concavity	-0.7715
r <sup>2</sup>	0.01521	r <sup>2</sup>	0.04147
modeled steepness (log)	0.7369	modeled steepness (log)	0.8751
modeled steepness	5.4563	modeled steepness	7.5007
<b>James north</b>		<b>James north</b>	
raw steepness (log)	0.1316	raw steepness (log)	0.9245
raw steepness	1.3538	raw steepness	8.4052
concavity	-0.4064	concavity	-0.54317
r <sup>2</sup>	0.01543	r <sup>2</sup>	0.02440
modeled steepness (log)	0.6873	modeled steepness (log)	0.6701
modeled steepness	4.8674	modeled steepness	4.6784

Table 4. Comparison of longitudinal profile modeling for 10m resolution data and 30, resolution data for the same basin.

<b>Lehigh west 30m – all streams</b>		<b>Lehigh west 10m – all streams</b>	
raw steepness (log)	-2.3968	raw steepness (log)	-2.8273
raw steepness	4.011e-3	raw steepness	1.488e-3
concavity	-0.04543	concavity	0.05764
r <sup>2</sup>	9.376e-4	r <sup>2</sup>	3.749e-4
modeled steepness (log)	-2.397	modeled steepness (log)	0.5103
modeled steepness	4.009e-3	modeled steepness	3.2382
<b>Lehigh west 30m – shale streams</b>		<b>Lehigh west 30m - shale streams</b>	
raw steepness (log)	-2.7111	raw steepness (log)	-3.6440
raw steepness	1.945e-3	raw steepness	2.270e-4
concavity	0.02185	concavity	0.2065
r <sup>2</sup>	2.5046e-4	r <sup>2</sup>	5.71052e-3
modeled steepness (log)	0.2682	modeled steepness (log)	0.5996
modeled steepness	1.8544	modeled steepness	3.9774



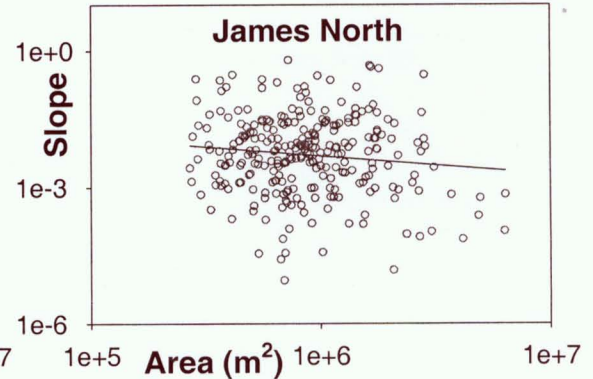
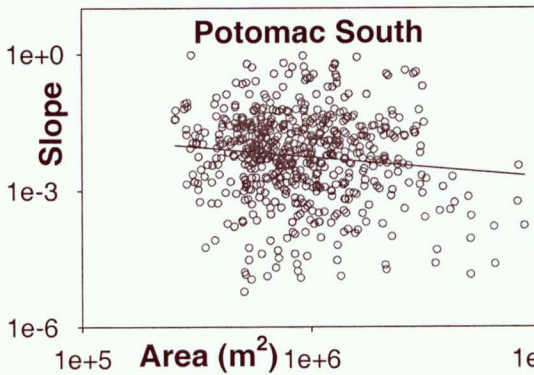
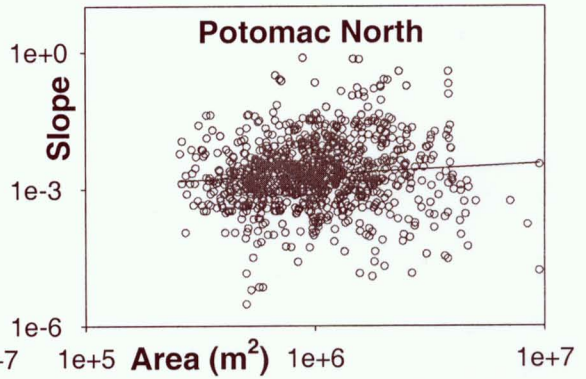
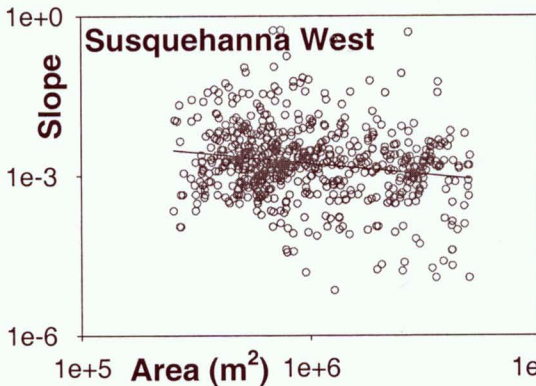
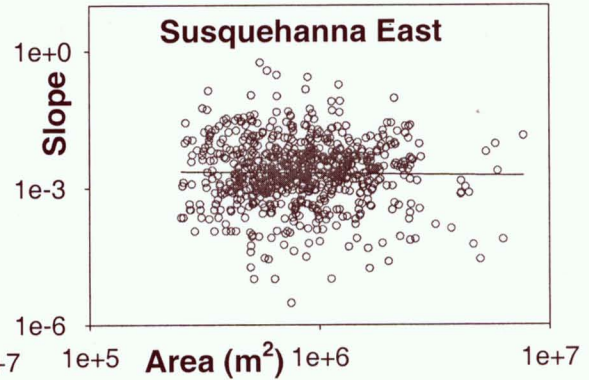
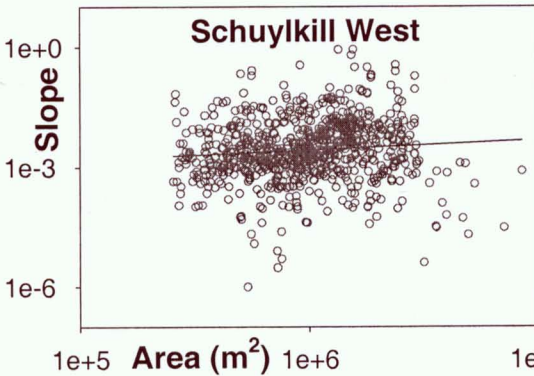
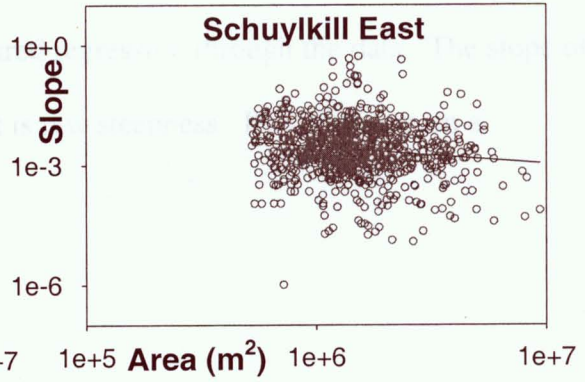
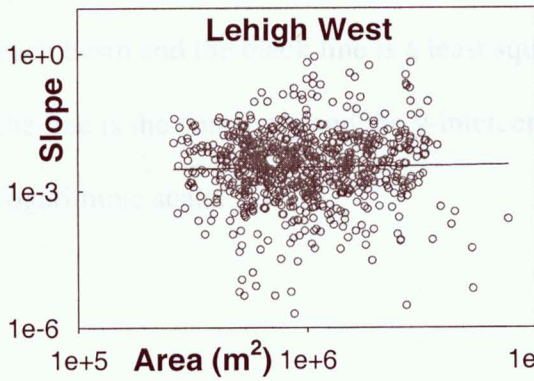


Figure 14. Black circles show the area-slope pairs for all of the first order streams in each basin and the black line is a least squared regression through the data. The slope of the line is the concavity and the y-intercept is raw steepness. Both axes are on a logarithmic scale.

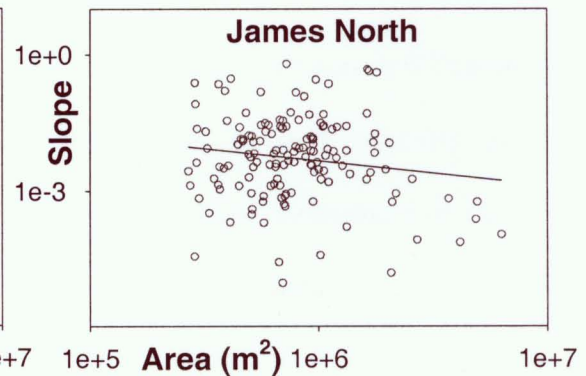
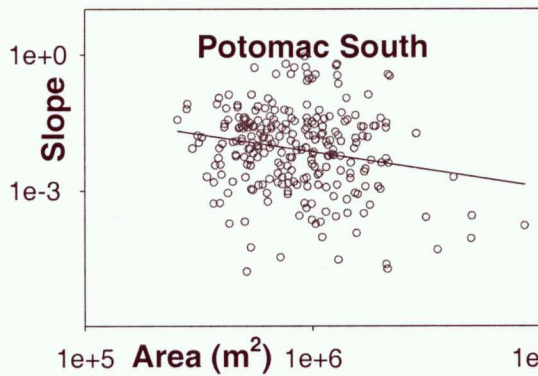
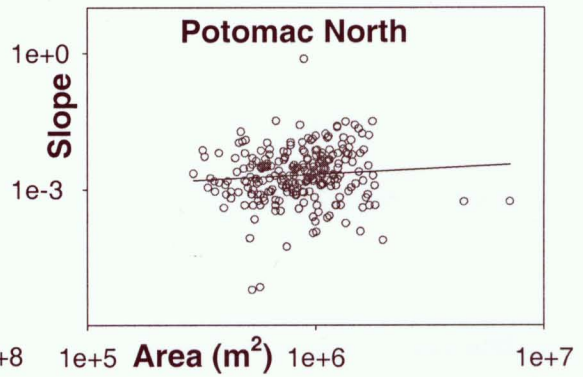
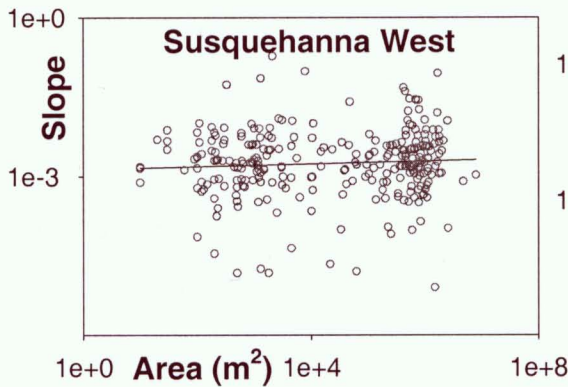
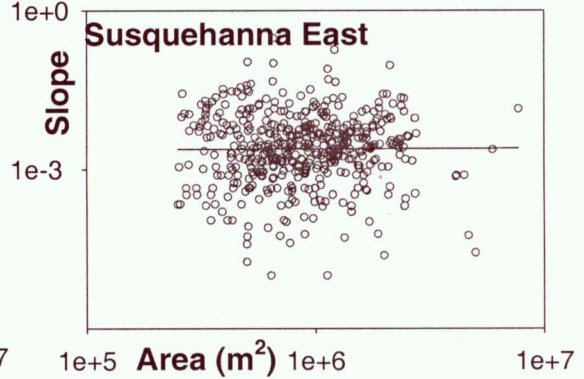
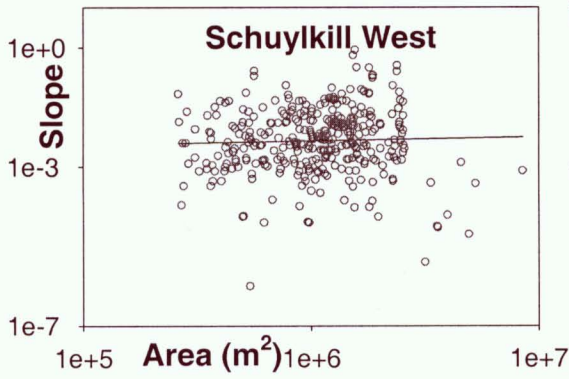
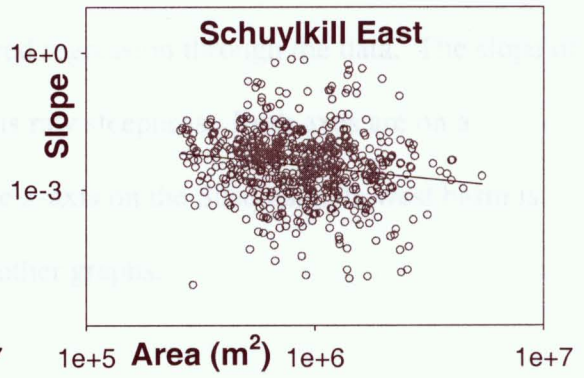
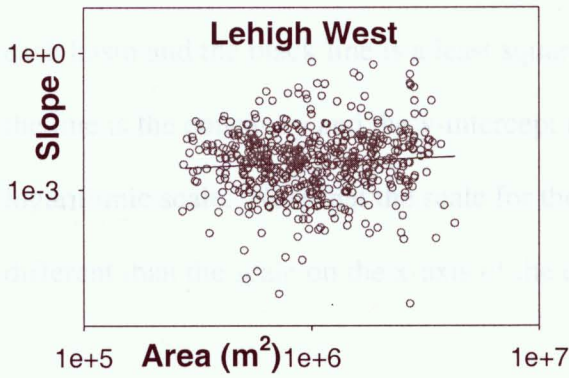


Figure 15. Black circles show the area-slope pairs for the shale first order streams in each basin and the black line is a least squared regression through the data. The slope of the line is the concavity and the y-intercept is raw steepness. Both axes are on a logarithmic scale. Note that the scale for the x-axis on the Susquehanna west basin is different than the scale on the x-axis of the other graphs.

## **Discussion**

The long term evolution of the Great Valley can be reconstructed from an analysis of upland gravel deposits and the metrics of first-order streams present at the watershed divides of the major transverse drainage of the Atlantic slope. Control of these divides may depend on a sensitive adjustment to rock type (Braun, 1983) and climate (Zaprowski et al., 2005) or base level (Powell, 1875), either local, regional or ultimate. Ultimately, these data can then be reconciled with the concepts of impulsive uplift and peneplanation (Davis 1889) and dynamic equilibrium (Hack 1960).

### *Upland gravels and origin of the current drainage divide*

The presence of upland gravel deposits in a divide area are interpreted in terms of the relative mobility and evolution of the divide as the first order streams, which currently flank these divides, are not responsible for the deposits. In fact, most divides have a scarcity of cobbles that argue for either originally small deposits or poor preservation of initially larger, more widespread deposits. In contrast, the modern fluvial system in the Cumberland Valley has extensive fluvial deposits preserved as terraces along the major strike parallel, trunk streams. Cobbles collected from each upland deposit were analyzed for provenance. Unfortunately, the two main source rocks for cobbles in upland deposits of the Great Valley, the Antietam Quartzite, and Tuscarora Sandstone, look very similar in hand sample: both are white to tan in color (fig. 3). Only one of the deposits identified in this study, the Orchard deposit, contained distinct clasts of Juniata Sandstone, which is characteristically purple. Thin sections (fig. 11) made from cobbles from each of the deposits showed that all but one of the cobbles are

sandstone consisting of cemented, metamorphosed quartz grains. Both the Antietam Quartzite and Tuscarora Sandstone are composed of metamorphosed quartz. The Roxbury Rd. (map plate 1) deposit contained a metamorphosed cobble, which indicated that it had its source in South Mountain and the Antietam Quartzite. *Skolithos*, a trace fossil, was found in several cobbles from the Salem deposit. *Skolithos* is prevalent in the Antietam Sandstone but can also be found in the Tuscarora Sandstone.

It is possible to conclude that the source of the Roxbury Rd. deposit was in part from South Mountain and that the source for the Orchard deposit was in part from Blue Mountain. Otherwise, concluding the source of any one deposit with certainty is not possible. Cobble shape is indicative of function, the shape of the cobble is directly influenced by the process by which it was formed. The Flinn diagram of average cobble shape (fig. 7) shows that most of the deposits and modern stream samples are clustered around the one to one line. The Salem deposit lies outside of this cluster as being, on average, more prolate. The next most prolate samples are both from modern streams fed by Blue Mt. and composed of gravels from Blue Mt. The Salem deposit is high in the landscape (~760ft asl) compared to the other deposits. Surficial deposits, higher in the landscape are older, thus, the Salem deposit may be a pre-Quaternary deposit while the other gravel deposits, which more closely resemble modern streams are Quaternary in age. The Salem deposit may be a deposit from one of the strike parallel streams, as it is in the middle of the valley, while the other deposits may be relicts of feeder streams coming off either Blue or South Mts., as they are closer to the flanks of the Great Valley. This difference may explain the difference in average shape between Salem and the other deposits. Additionally, as the deposits become younger they probably have stronger

periglacial influence than older deposits. Evidence from these upland deposits does not suggest watershed expansion of the large transverse rivers of the Atlantic margin at the expense of others. Additionally, all but one of the deposits, Orchard, is found on carbonates. Lowering of the landscape through dissolution rather than erosive transport, which is dominant on the shale lithologies, may allow for the preservation of upland deposits. The sedimentology of each deposit is indicative of an integration of drainage from both South and Blue Mts. by both river and fan deposits but not of a dynamically shifting divide driven by differences in the regional base level controlled by the major transverse drainages. Over time, drainage systems migrate within an overall stationary system and ultimately leave formerly topographically low cobble deposits at high points in the divide area.

#### *Mobility of the drainage divide inferred from stream long profiles*

Slope-area modeling of stream longitudinal profiles has proven to be a useful tool in quantifying the rate of rock uplift and subsequent river incision in tectonically active settings (Duvall, 2004; Merritts, 1989; Molin et al., 2004; Snyder, 2000; Whipple, 2004). Given the key assumption of equilibrium profiles, which are attainable in tectonically active regions where surface processes are rapid, this study embarks on a test to see how well the method performs in the tectonically stable setting where surface process rates are slow, and disequilibrium persists in the profile for long periods of time. In summary, modeled long profiles in the low-gradient channels of Great Valley divides generated data with a high degree of scatter and with few apparent trends within a single basin or among comparable basins (figs. 14 and 15). The lack of trends could be due to two major

factors; (1) streams in this study violate the assumption of equilibrium inherent in the logA-logS method or (2) the channel slopes of the study area are too gentle to be uniquely discernable on logA-logS plots.

A river long profile is said to be in equilibrium when the incision is everywhere uniform and the rate is both steady and equal to the rate of rock uplift. In the Great Valley, the fluvial incision is directly related to base level fall, namely that of the master transverse Atlantic Slope rivers. Landscape erosion is throttled by changes in base level but translation of this signal upstream as fluvial incision is not immediate or linear. Translation of base level fall can be envisioned evolving in two ways; an overall steepening of the channel as the nickzone lays back, or as an incisional wave that marches headward as a steep, parallel retreating nickzone (Gardner, 1983). Both processes should affect the concavity ( $\theta$ ) and overall steepness ( $k_s$ ) of modeled long profiles.

An increase of channel steepness would not necessarily lead to increased scatter in a logA-logS plot but would help define a relationship between logArea and logSlope. Knickzones leave channels in a state of disequilibrium. Knickzones represent a transient state of incision between the reach below and above the knickzone. With the introduction of several falls in base level and the translation of these events upstream, as nickzones, a complicated set of channel reaches unfolds, each out of equilibrium with other portions of the channel creating a series of different regional base levels and each out of phase with ultimate base level as well. Additionally, it is possible for knickpoints to stall indefinitely at one location. Introduction of one or more base level falls in the form of knickpoints can leave channels in a complex state of disequilibrium, violating



one of the assumptions of the method, and may cause increased scattered in logA-logS plots.

The James, Potomac and Susquehanna Rivers, three transverse rivers which drain the Great Valley, have disequilibrium long profiles as demonstrated by numerous nickzones, overall convex lower reaches (Pazzaglia et al., 1998), and unsteady incision (Pazzaglia and Gardner, 2003; Reusser et al., 2004). These trunk channels are not in equilibrium, a condition that appears to persist into the major tributaries of these streams based upon the average steepness and concavity of areas.

The data do not suggest that a singular factor such as regional base level controls all of the first order streams in a single basin, let alone more than one basin. Highly variable logA-logS plots (Figs. 13 and 14), with low  $r^2$  values (tables 2 and 3) for regression lines, yielded from the longitudinal profile modeling do not suggest first order streams that are in equilibrium with trunk channels. Low initial slope values are one reason for poorly correlated data but in this case, there seems to be very little change in the slope of a first order stream based on its upstream drainage area. The data for modeled steepness values for first order streams from two different basins, which eventually drain into the same transverse drainages (regional base level), are no more similar than the steepness values for any two of the basins studied despite to which transverse river they are tributary.

Variable slope-area plots fuel an investigation into what is causing the apparent disequilibrium in Appalachian first-order channels. It is known that climate, for example, affects the equilibrium condition and evolution of long profiles (Roe et al., 2002; Whipple, 2004; Zaprowski et al., 2005). A wetter climate produces stream channels with

increased concavity and eventually lower steepness values, opposite the effect of base level fall because of the large increase in discharge down stream. A dryer climate will produce opposite results, which mimic the effects of a base level fall. Climatic differences between the basins within the Great Valley are small as the entire study area is within the temperate zone of the Koeppen classification system (Ritter 2003).

If climatic factors control differences in concavity and steepness values between the basins of the Great Valley then we would expect that basins that share a divide would be more similar to each other than divides of separate basins. The northern six basins (fig. 2) have positive concavity values for the shale streams indicating that the first order channels in these basins have convex profiles. These basins all have values that fall between 0.01251 and 0.5234 (table 2) but show no trends. The southern two basins (fig. 2), Potomac south and James north, which share a divide have negative concavity values for the shale streams indicating that the first order channels in the these basins have a concave profile. Similarly, the northern six basins have modeled steepness value which range from 1.7179 to 3.2382 (table 2) for all streams and from 0.2689 to 4.6484 (table 2) for the shale streams. The two southernmost basins have modeled steepness values of 5.45634 and 4.8674 (table 2) for all the first order streams in the Potomac south and James north, respectively. Modeled steepness values for just the shale streams of 7.5007 and 4.6784 (table 2) of the Potomac south and James north, respectively, are similarly higher than modeled steepness values of shale streams from the northern six drainages, which range from 4.6484 to 0.2689 (table 2). Upon examination of the long profile modeling values, especially those which considered only shale streams, the James north and Potomac south basins show consistently higher steepness values, in some cases

almost double, while the northern six drainages fall within the noise of any natural system. The concavity values of the shale channels show a clear change in channel shape between the two southernmost drainage and the six northern drainages. Unfortunately, there is the complicating factor of different resolution DEM between these basins and the other basins. The steepness values for the Lehigh west basin are lower when they were modeled from the 30m data rather than the 10m data indicating that, if the data are not comparable, at least it is known that the 30m data yields an underestimate for steepness values. Intriguingly, the hypsometric plots for all of the basins show that basins have hypsometries similar to the basin with which they share a divide rather than the basin with which they share a regional base level. Modeling and whole basin metric data indicates a connection between the James north and Potomac south drainage basins. Modern incision rates for the James, between 160m/my (Harbor 2000) and 110m/my (Ries 1998), and Potomac Rivers, 10-20m/my (Ruesser 2004), indicate that first order streams flanking the divide are not controlled by differential incision rates of these two large rivers. There are two possible reasons for the first order streams to be out of equilibrium with their regional base levels; either the base level signal has not been translated to these streams yet; or there is another factor such as bedrock or climate that is controlling steepness, concavity and hypsometry.

The assumption of equilibrium requires that tectonic forces of uplift are equal to erosional forces of downcutting. Tectonic forces in the Great Valley and on the Atlantic margin are virtually non-existent. Isostatic forces in the Great Valley are minimal and limited to glacial rebound, forebulge, and long term uplift due to erosion. These factors are low magnitude forces which affect large regions (glacial forebulge and rebound) or

the entire Atlantic margin (long term uplift). Additionally, the time scale on which glacial factors have an effect are smaller than the time scale of the landscape evolution of the Great Valley, whereas, uplift due to erosion has continued from the opening of the Atlantic.

## **Conclusions**

Landscape morphology within the Great Valley is delicately adjusted to rock type and climate rather than base level. Low order streams flanking the divides between the major transverse drainages are similar in shape and steepness to streams in adjacent divides. Over time, these streams tend to have a concave rather than convex shape (fig. 16). Drainage networks in the Great Valley are organized to move water from the divide areas through subsequent, strike parallel, drainages to consequent, transverse, drainages and eventually to the Atlantic Ocean. The system will naturally change in order to allow the water to move to base level as quickly as possible. The purpose of this study was to determine whether a competitive advantage in any one of transverse drainage system was driving drainage capture and divide migration within the Great Valley. The progressive breaching, which is supported by modern incision rates, of the Great Valley by the Susquehanna River, then the Potomac River and finally the James river as indicated by increasing current incision rates does not seem to have affected the divide areas between these rivers in the Great Valley. Additionally, this study attempted to reconcile the paradigms of dynamic equilibrium (Hack) versus orogenic impulse and decay (Davis).

- Evidence from upland gravel deposits in the Cumberland Valley does not suggest active divide migration and drainage expansion of one master

drainage at the expense of another. Gravel deposits indicate the integration of South and Blue Mt. drainages with the eventual inversion of topography over a long period of time.

- Similarly to the transverse drainages of the Great Valley, channel metrics of the strike parallel drainages from longitudinal profile modeling suggest systems in disequilibrium with base level that are sluggishly connected to changes in base level.
- Despite disequilibrium in the system, the channels flanking either side of the divide between the James and Potomac Rivers have higher average concavity and steepness values. In conjunction with the hypsometric plots from all basins, there is the suggestion of a stronger connection between basins that share a divide than basins that share a base level.
- Suggestions of connections between strike parallel basins may exist but the logA-LogS method is insensitive. Ultimately, in this low slope environment, modeling longitudinal profiles using the logA-logS method is inadequate.

Upland gravel data supports a steady lowering of the landscape rather than divide mobility. Insensitivity of slope to upstream drainage area, indicating a system ill adjusted to base level and connection of basins across divides rather than between transverse drainages supports the concept that the landscape of the Great Valley is adjusted to climate and rock type rather than regional base level. In the Davisian model, the steeper slopes and convexity of the James north and Potomac south drainages indicate a more recently incised landscape as compared to the drainages further to the north.

Unfortunately, DEMs, even with 10m resolution proved to be insensitive to the low relief in the landscape of the Great Valley adding noise to the system and hindering the interpretations. Ultimately, based on the data collected, Davis' model of erosional decay following landscape perturbation (rock uplift or base level fall) better describes the landscape evolution of the Great Valley.

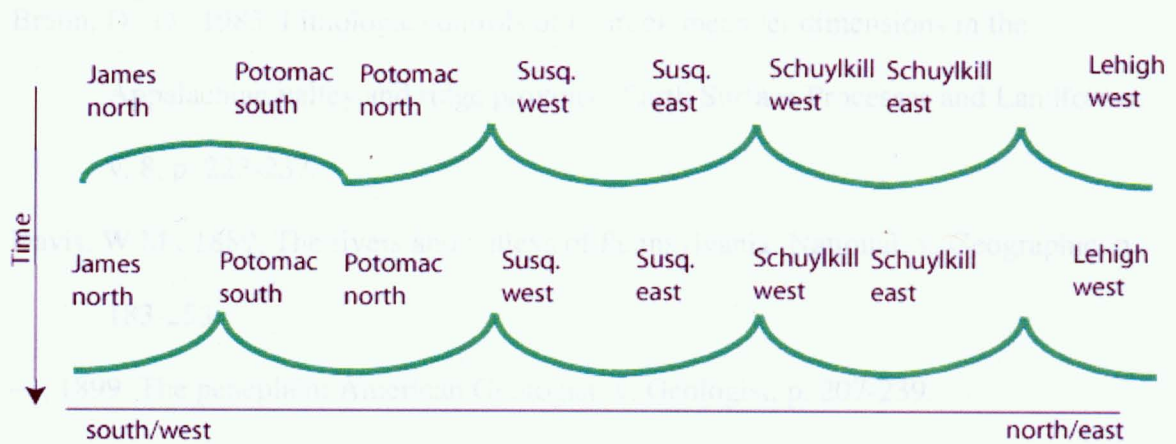


Figure 16. A schematic diagram showing an interpretation of future landscape evolution in the Great Valley. Over time the divide between the James and Potomac rivers will become concave up like the divides between the other transverse drainages rather than convex.

## References

- Bagnold, R., A., 1973, The nature of saltation and of bedload transport in water:  
Proceedings of the Royal Society of London, v. ser. A, p. 473-504.
- , 1977, Bed-load transport by natural rivers: Water Resources Research, v. 13, p. 303-312.
- Braun, D., D., 1983, Lithologic controls of bedrock meander dimensions in the Appalachian valley and ridge province: Earth Surface Processes and Landforms, v. 8, p. 223-237.
- Davis, W.M., 1889, The rivers and valleys of Pennsylvania: National, v. Geographic, p. 183-253.
- , 1899, The peneplain: American Geologist, v. Geologist, p. 207-239.
- Duvall, A., Kirby, E., Burbank, D., 2004, Tectonic and lithologic controls on bedrock channel profiles and processes in coastal California: Journal of Geophysical Research, v. 109, p. doi:10.1029/2003Jf000086.
- Gardner, T.W., 1983, Experimental study of knickpoint and longitudinal evolution in cohesive, homogeneous material: Geological Society of America Bulletin, v. 94.
- Gilbert, G.K., 1877, Report on the Geology of the Jenry Mountains: Washington D.C., Government Printing Office.
- Glock, W.S., 1931, The development of drainage systems: A synoptic view: Geography Review, v. 21, p. 475-482.
- Hack, J.T., 1960. Interpretation of erosional topography in humid temperate regions: American Journal of Science, v. 258-A, p. 80-97.
- , 1982. Physiographic divisions and differential uplift in the Piedmont and Blue Ridge.

- Hancock, G.S., Harbor, D. J., Felis, J., Turcotte, J., 2004,  $^{10}\text{Be}$  Dating of river terraces reveals piedmont landscape disequilibrium in the central James River basin, Virginia: Geological Society of America Abstract with Programs, v. 36, p. 95.
- Harbor, D., 2000, Landscape evolution in the Upper James River basin, *in* Harbor, D., ed., Southeastern friends of the Pleistocene: Washington and Lee University, Lexington , VA.
- Hulver, M.L., 1992, Mass balance and the long term denudation of the Appalachians: Geological Society of America Abstract with Programs, v. 24, p. 237.
- , 1996, Post Orogenic denudation and mass-balances topography of the Appalachian Mountain system from maturation indicators, thermochronology, and metamorphic petrology.: Geological Society of America Abstract with Programs, v. 28, p. 500.
- Jacobsen, E.F., and Lyons, P.C., 1982, Stratigraphy, structure, and coal-bed correlations in the Castleman Basin, Garrett County, Maryland: Abstracts with programs, Northeastern and Southeastern combined section meetings Abstracts with Programs - Geological Society of America, v. 14, p. 28.
- Long, R.S., 1975, Soil Survey of Franklin County, Pennsylvania, United States Department of Agriculture Soil Conservation Service.
- Merritts, D.J., Vincent, Kirk R., 1989, Geomorphic response of coastal streams to low, intermediate and high rates of uplift, Mendocino triple junction region, northern California: GSA Bulletin, v. 101, p. 1373-1388.
- Molin, P., Pazzaglia, F.J., and Dramis, F., 2004, Geomorphic expression of active tectonics in a rapidly-deforming forearc, sila massif, calabria, southern Italy: American Journal of Science, v. 304, p. 559-589.



- Pazzaglia, F.J., and Brandon, M.T., 1996, Macrogeomorphic evolution of the post-Triassic Appalachian mountains determined by deconvolution of the offshore basin sedimentary record: *Basin Research*, v. 8, p. 255-278.
- Pazzaglia, F.J., Gardner, T.W., 2003, Late Cenozoic landscape evolution of the US Atlantic passive margin; insights into a North American Great Escarpment, *in* Summerfield, M.A., ed., *Geomorphology and global tectonics*: Chichester, John Wiley & Sons.
- Pazzaglia, F.J., Gardner, T.W., Merritts, D.J., 1998, Bedrock Fluvial Incision and Longitudinal Profile Development Over Geologic Time Scales Determined by Fluvial Terraces, *in* Tinkler, K.J., Wohl, E., ed., *Rivers Over Rock: Fluvial Processes in Bedrock Channels*, Volume 107: Washington D.C., American Geophysical Union.
- Pierce, K. L., 1965, Geomorphic significance of a Cretaceous deposit in the Great Valley of southern Pennsylvania: U. S. Geological Survey Professional Paper 525-C, p. C152-C156.
- Potter, N., 2001, The Geomorphic Evolution of the Great Valley near Carlisle, Pennsylvania, Southeast Friends of the Pleistocene: Carlisle, Pennsylvania.
- Powell, J.W., 1875, *Exploration of the Colorado River of the West*: Washington D.C., U.S. Government Printing Office, p. 291.
- Reusser, L.J., Bierman, Paul R., Pavich, Milan J., Zen, E-an, Larsen, Jennifer, Finkel, Robert, 2004, Rapid Late Pleistocene Incision of Atlantic Passive-Margin River Gorges: *Science*, v. 305, p. 499-502.

- Reuter, J.M., Beirman, P. R., Pavich, M., Gellis, A. C., Larsen, J., Finkel, R. C., 2004, Erosion of the Susquehanna River basin: Assessing the relations between 10Be-derived erosion rates and basin characteristics: Geological Society of America Abstract with Programs, v. 36, p. 94.
- Ries, J., Merritts, D., Harbor, D. J., Gardner, T., Erikson, P., Carlson, M., 1998, Increased rates of fluvial bedrock incision in the Central Appalachian Mountains, Virginia: Geological Society of America Abstract with Programs, v. 30, p. 140.
- Ritter, M., 2003, The Physical Environment:  
[http://www.uwsp.edu/geo/faculty/ritter/geog101/textbook/title\\_page.html](http://www.uwsp.edu/geo/faculty/ritter/geog101/textbook/title_page.html).
- Roe, G.H., Montgomery, D.R., and Hallet, B., 2002, Effects of orographic precipitation variations on the concavity of steady-state river profiles: *Geology (Boulder)*, v. 30, p. 143-146.
- Schultz, C.H., 1999, *The Geology of Pennsylvania*: Harrisburg, Pennsylvania Geological Survey and Pittsburgh Geological Survey.
- Schumm, S.A., and Rea, D.K., 1995, Sediment yield from disturbed earth systems: *Geology (Boulder)*, v. 23, p. 391-394.
- Sevon, W.D., 1989, Erosion in the Juniata River Drainage Basin, Pennsylvania, *in* Gardner, T.W., Sevon, W.D., ed.. *Appalachian Geomorphology, Volume 2*: New York, Elsevier, p. 303-318.
- Snyder, N.P., Whipple, K. X., Tucker, Gregory E., Merritts, Dorothy J., 2000. Landscape response to the tectonic forcing: Digital elevation model analysis of stream profiles in the Mendocino triple junction region, northern California: *GSA Bulletin*, v. 112, p. 1250-1263.

- Strahler, A.N., 1952, Hypsometric (area-altitude) analysis of erosional topography: GSA Bulletin, v. 63, p. 1117-1142.
- Whipple, K.X., 2004, Bedrock rivers and the geomorphology of active orogens: Annual Review of Earth and Planetary Sciences, v. 32, p. 151-185.
- White, W.B., 1984, Rate processes: chemical kinetics and karst landform development, *in* LaFleur, R.G., ed., Groundwater as a geomorphic agent: Boston, Allen and Unwin, p. 227-248.
- , 2000, Dissolution of limestone from field observations,, *in* Kimchouk, A.B., Ford, D. C., Palmer, A. N., and Dreybrodt, W., ed., Speleogenesis, evolution of karst aquifers, Volume January 2000, National Speleological Society.
- Zaprowski, B.J., Pazzaglia, F.J., and Evenson, E.B., 2005, Climatic influences on profile concavity and river incision: Journal of Geophysical Research-Earth Surface, v. 110.
- Zarichansky, J., 1986, Soil Survey of Cumberland and Perry Counties, Pennsylvania, United States Department of Agriculture Soil Conservation Service.

## Appendix A– Upland Gravel Data

### KEY

\*All numerical measurements are in millimeters.

Color:	Rock Type:	Weathering:
p-pink	l - limestone	1 - least weathered
r-red	s - sandstone	7 - most weathered
b-black	m - mudstone	
br-brown	q - quartzite/quartz sandstone	
u-purple		
t-tan		
w-white		
g-gray		
e-green		

### Roxbury Rd.

A-axis	B-axis	C-axis	avg. rind thickness	color	rock type	weathering	fabric
144.6	84.7	76.5	2.1	t	s	3	n
60.5	59.5	36.4	1.2	r/t	q	4	n
81.8	62.4	46.6	3.6	w	q	4	n
62.2	49.1	25.6	2.55	p	q	3	n
79.7	71.8	41.2	6.85	t/b	s	4	y
60.9	51	36.2	4.9	p	q	3	n
33.7	27.4	22.9	2.6	p/t	s	3	y
35.9	23	18.9	3.3	w	q	4	y
52.3	55.4	48.8	1.6	t	q	3	n
60.1	58.9	30.6	3.1	p	s	4	n
46.1	35	26.6	2.4	w/b	q	3	n
45.9	32.7	22.4	1.8	r/w/b	q	4	n
46.3	27	22.1	0	t	q	3	n

### Frecon Rd.

A-axis	B-axis	C-axis	avg. rind thickness	color	rock type	weathering	fabric
141.1	95.5	26.2	0	w	q	4	n
73.2	72	51.9	3.3	p/w	s	3	y
117.4	72.2	48.3	1.6	t	s	3	n
74.3	54.8	44.4	0	t	s	3	n
58.9	40.5	23.4	4.9	g	s	4	n
90.2	62.7	32	5.1	p	s	3	n
91.7	76.6	35.1	2.9	w/b	s	3	y

80.2	65.1	41.3	2.3	p/b	s	3	y
65.9	39.4	27.9	0	r	q	4	n
108.6	96.3	69	2.1	t	s	3	n
91.1	86.5	54.3	2.4	w	s	3	n
73.4	52.7	38.6	3.4	g	q	3	n
96.3	78.2	51.4	0	w	q	2	y
135.8	54.5	41	2.5	p	s	3	n
47.2	44.9	22.2	0	t	q	3	n
67.5	59.4	48.1	2.6	p	s	3	n
48.3	32.1	22.1	2.5	p	s	3	n
86.2	60.5	36	0	p	q	4	n
49.3	40.3	33.5	1.4	t	s	3	n
98.7	31.5	27.7	3.3	t	s	3	n
96.4	87.8	26.4	0	t	s	3	y
56.3	56.2	20.2	1.3	t	s	3	y

### Beistle

A-axis	B-axis	C-axis	avg. rind thickness	color	rock type	weathering	fabric
105.5	77.7	48.2	1.1	w/t	s	5	n
106.6	56.1	52.6	2	p	s	3	n
132.5	94.3	55.1	3.2	bl-br	s	3	y
107.1	62.1	41.4	6.3	w	s	3	y
21	18.1	13	1.5	t	s	3	y
103.9	95.7	51.4	3	p	s	3	n
48.2	34.3	28.1	2.8	w/b	q	4	n
66.3	42.4	40.3	2.9	t/w	s	3	y
58.6	38	31.6	7.4	w	s	3	n
62.4	40	25.3	1.1	br	s	4	n

### Salem

A-axis	B-axis	C-axis	avg. rind thickness	color	rock type	weathering	fabric
78.4	54.7	49.3	0	w	q	2	n
149.2	87.8	64.4	3.7	g	q	3	y
73.1	58.2	36.2	3	w/b	s	4	n
94.5	40.2	35.4	0	r	s	3	n
126	79.8	43.7	2	g/w	s	3	n
78.2	64.9	38	4.1	p/t	s	3	n
94.8	76.8	47.3	1.3	w	s	4	y
82	43.8	23.1	0	t	q	2	y
88.3	55.2	46.3	0	b/t	s	5	n
95.9	85.1	54.8	0	t	s	3	n

115.5	56.3	36.1	3	b	q	5	n
128.7	73.1	39.6	2.8	w/p	q	3	y
122	56.3	39.9	7	br	s	3	n
56.8	57.9	41.5	0	t	q	3	n
72.3	42	24.2	2.4	w/b	s	3	n
67.9	51.7	51.4	5.4	p/b	s	3	y
71.9	64.3	33.3	0	w	s	3	y
76.6	50.1	39.6	1.5	p	s	3	y
58.5	27.7	19.3	2.7	w/b	q	4	y
47.4	33.4	29.9	0	w/r	s	3	n
52.1	50	26.3	0	w	s	3	n
77.6	59.8	22	0	w	q	3	n
56.8	40.9	25.5	1.6	r	s	3	n
56.8	46.9	22	2.4	p/w/br	q	4	y
58.6	40	23.9	0	w	s	3	n
52.1	38.8	29.8	0	w	q	2	n
55.1	39.4	37.9	2.2	w	q	2	y
49.3	49.2	24.8	3.9	w/b	s	4	y
91.9	60.7	60.4	0	w	s	3	n
72.5	44.5	43.3	1.9	w	q	2	n
55.9	32.8	22.5	0	w	q	2	n
70.1	36.2	28.9	0	t	q	3	n
72.1	54	20.8	1.9	t/b	s	3	y
76.5	51.9	51.5	1.7	t	s	3	n
73.3	54.1	37.6	2.5	w	s	3	n
92.9	56.2	53.9	0	t	s	3	n
70.4	41.7	37.5	0	t	s	3	n
42.9	25.3	18.5	0	t	s	3	n
67.8	45.7	26.5	0	t	s	3	n
50.2	31.6	30.3	0	w	q	2	y
71.2	48.2	20.4	1.4	w/b	s	3	n
63.1	55.8	11.7	0	p	q	2	n
58.8	43.6	36.1	2	w/b	s	3	n
58.1	46.4	35.9	2.1	br	s	3	y
61.2	51.1	15	2	t	s	3	n
61	47.4	27.6	1.2	w	s	3	n
46.6	34	32.8	0	w	s	3	n

### Orchard

A-axis	B-axis	C-axis	avg. rind thickness	color	rock type	weathering	fabric
67.5	47.4	23.5	2.4	u	s	3	n
73.2	46.1	40.5	3.8	p/t	s	5	n

107.4	95.5	65	4.9	t/br/r	s	3	n
77.7	75.7	53.9	0	w/b/r	s	2	n
67.4	66.8	53.5	2.6	u	s	3	n
121.5	46	32.8	3.7	r/b	s	2	n
93.1	73.9	23	5.5	w	s	2	n
87.1	51.7	43.6	1.6	t	s	2	n
92.2	68.7	51.2	0	w/t	s	6	n
47.8	39.6	11.6	1.3	t	s	3	n
69.2	39.5	21.5	0	b/p	s	2	n
81	51.8	22.7	2.7	r/b	s	2	n
62.7	60.5	3.63	1.6	t	s	3	n
45.5	42.5	29.2	0	w/t	s	3	n
65.7	53	32.7	0	u	s	3	n
75.9	52	26.7	1.7	t	s	3	n
57.4	48.8	23.5	6.1	t	s	3	n
70.5	39.3	35.9	0	t	s	3	n
50.6	39.3	16.8	1.4	t	s	3	n
33.9	28.6	27.1	1	t	s	3	n
57.3	41.2	27.5	1.3	t	s	3	n
39.2	29.2	17.7	3.2	u/r	s	4	n
54.9	48.6	29	1.3	t	s	3	n
57.4	49	21.3	2.9	w	s	3	n
62	35.9	13	0	b/w/r	s	3	n
36.6	19.3	18.5	3.3	u	s	3	n
53.1	35.1	15.4	0.5	t	s	3	n
49.2	39.2	37.2	0	t	s	3	n

### Mainsville Quarry

A-axis	B-axis	C-axis	avg. rind thickness	color	rock type	weathering	fabric
65.1	51.6	26.6	N/A	t/r	Saprolite	7	N/A
123.4	75.5	41.1	N/A	t/r	Saprolite	7	N/A
88.6	61	55	N/A	t/r	Saprolite	7	N/A
137.5	101.5	34.8	N/A	t/r	Saprolite	7	N/A
131.5	120.9	45.6	N/A	t/r	Saprolite	7	N/A
100.6	70.6	33.4	N/A	t/r	Saprolite	7	N/A
101.6	64.7	64.2	N/A	t/r	Saprolite	7	N/A
94.5	73	50.3	N/A	t/r	Saprolite	7	N/A
104.7	72.8	49.1	N/A	t/r	Saprolite	7	N/A
95.8	58.5	57.2	N/A	t/r	Saprolite	7	N/A
104.4	92.3	35	N/A	t/r	Saprolite	7	N/A
87.3	77	28.1	N/A	t/r	Saprolite	7	N/A
81.8	57.3	39.6	N/A	t/r	Saprolite	7	N/A
104	74.5	47.7	N/A	t/r	Saprolite	7	N/A

88.7	59	47.2	N/A	t/r	Saprolite	7	N/A
94.5	71.6	46.7	N/A	t/r	Saprolite	7	N/A
86.2	68.8	47.7	N/A	t/r	Saprolite	7	N/A
76.2	60.8	41.4	N/A	t/r	Saprolite	7	N/A
89.8	75.3	40.3	N/A	t/r	Saprolite	7	N/A
101.7	68.1	48	N/A	t/r	Saprolite	7	N/A
91	51.3	27.9	N/A	t/r	Saprolite	7	N/A
76.5	44.7	37.2	N/A	t/r	Saprolite	7	N/A
69.6	68.3	57.3	N/A	t/r	Saprolite	7	N/A
86.3	48.6	30.1	N/A	t/r	Saprolite	7	N/A
73	39.3	31.4	N/A	t/r	Saprolite	7	N/A
82.8	68	44.5	N/A	t/r	Saprolite	7	N/A
85.9	69	48.4	N/A	t/r	Saprolite	7	N/A
76.2	69.2	51.4	N/A	t/r	Saprolite	7	N/A
93.4	75	25	N/A	t/r	Saprolite	7	N/A
61.5	40.8	37.4	N/A	t/r	Saprolite	7	N/A
74.9	57.8	30.5	N/A	t/r	Saprolite	7	N/A
68.1	40.3	27.4	N/A	t/r	Saprolite	7	N/A
85.2	47.2	26.8	N/A	t/r	Saprolite	7	N/A
84.2	51.4	25.8	N/A	t/r	Saprolite	7	N/A
73.9	65.5	29.1	N/A	t/r	Saprolite	7	N/A
59.9	39.9	29.2	N/A	t/r	Saprolite	7	N/A
61.1	68.4	33.4	N/A	t/r	Saprolite	7	N/A
47.2	37.6	21.2	N/A	t/r	Saprolite	7	N/A
69.5	49	44.5	N/A	t/r	Saprolite	7	N/A
70.4	51	33	N/A	t/r	Saprolite	7	N/A
58.7	41.4	34.5	N/A	t/r	Saprolite	7	N/A
71.8	45.7	32.5	N/A	t/r	Saprolite	7	N/A
55.7	51	36.9	N/A	t/r	Saprolite	7	N/A
66.9	38.1	30.2	N/A	t/r	Saprolite	7	N/A
68.6	39.5	26.8	N/A	t/r	Saprolite	7	N/A
85.9	51.9	40.5	N/A	t/r	Saprolite	7	N/A
49.5	29.9	16.2	N/A	t/r	Saprolite	7	N/A
58.7	49	24.4	N/A	t/r	Saprolite	7	N/A
39.7	36.5	34	N/A	t/r	Saprolite	7	N/A
57	52.6	33.8	N/A	t/r	Saprolite	7	N/A
42.5	37	29.8	N/A	t/r	Saprolite	7	N/A
61.3	43	26.5	N/A	t/r	Saprolite	7	N/A
65.2	46.1	29.5	N/A	t/r	Saprolite	7	N/A
54.5	25.8	24	N/A	t/r	Saprolite	7	N/A
52.4	41.4	23.8	N/A	t/r	Saprolite	7	N/A
51.4	38.4	21.3	N/A	t/r	Saprolite	7	N/A
54.2	40.8	23.2	N/A	t/r	Saprolite	7	N/A
46.5	34.6	27.4	N/A	t/r	Saprolite	7	N/A
55.3	38.4	25.7	N/A	t/r	Saprolite	7	N/A



45.3	38.2	25.6	N/A	t/r	Saprolite	7	N/A
60.4	36	20.9	N/A	t/r	Saprolite	7	N/A
67.1	52	17	N/A	t/r	Saprolite	7	N/A
69.8	37.9	30.7	N/A	t/r	Saprolite	7	N/A
55	36.1	32.9	N/A	t/r	Saprolite	7	N/A
52.9	25.3	17.1	N/A	t/r	Saprolite	7	N/A
43.4	35.8	26.6	N/A	t/r	Saprolite	7	N/A
47	36.4	25.7	N/A	t/r	Saprolite	7	N/A
43.9	41.4	37.8	N/A	t/r	Saprolite	7	N/A
49.2	30.5	26.2	N/A	t/r	Saprolite	7	N/A
44.7	25.3	16.3	N/A	t/r	Saprolite	7	N/A
50.8	45.1	25.2	N/A	t/r	Saprolite	7	N/A
49.9	43.7	16.8	N/A	t/r	Saprolite	7	N/A
48.4	38	21.3	N/A	t/r	Saprolite	7	N/A
37.7	26.6	15.3	N/A	t/r	Saprolite	7	N/A
44.8	31.9	20	N/A	t/r	Saprolite	7	N/A
43.9	33.9	19.6	N/A	t/r	Saprolite	7	N/A
46	30.5	26.6	N/A	t/r	Saprolite	7	N/A
38.8	27.9	18.6	N/A	t/r	Saprolite	7	N/A
48.1	34.5	23.1	N/A	t/r	Saprolite	7	N/A
40.6	26.4	16.6	N/A	t/r	Saprolite	7	N/A
52	31.9	22.6	N/A	t/r	Saprolite	7	N/A
44.2	33.2	21.7	N/A	t/r	Saprolite	7	N/A
43.2	30.6	24.6	N/A	t/r	Saprolite	7	N/A
37.8	32.6	25.3	N/A	t/r	Saprolite	7	N/A
42.7	29	17	N/A	t/r	Saprolite	7	N/A

### Roxbury Gap

A-axis	B-axis	C-axis	avg. rind thickness	color	rock type	weathering	fabric
180	106.5	64.9	0	u	s	3	n
195	102.8	84.5	1.8	t/g	q	3	n
101.6	85.4	82	2.3	t/w	q	3	n
133.6	96.2	61.5	0	r	s	4	n
189	64.6	29.1	0	w	q	3	n
152.4	71.1	70.1	2	t	s	3	n
138	86.5	43.3	2.8	u	s	3	n
108	101.5	33.7	0	t/p	s	3	n
119	82.9	45.8	0	u	s	2	n
52.5	90	58.3	0	e	s	3	n
99.7	85.4	21.1	2.4	w	q	3	n
97	73.9	42.4	0	b	m	2	n
98.5	66.5	43.4	0	u	s	3	n
104.7	72.7	28.3	0	u	s	3	n

78.4	62.4	55.5	2.5	w	q	3	n
108.2	92.5	35.9	2	t	s	3	n
87.1	42.6	31.6	3.4	t/w	q	3	n
83	33	31.3	3.6	t	q	3	n
85.6	50.8	43.3	0	u	s	3	n
86.4	50.2	42.6	0	u	q	4	n
8704	28.9	24.6	1.9	w	q	3	n
111.7	46.1	37.6	1.5	g/t	s	3	n
92.6	32.2	31.1	5.5	w	q	3	n
94.2	53.4	12	4.4	t	s	5	n
70.7	60.3	36.4	2.8	t	q	3	n
59	49.5	25.7	4.5	t	q	3	n
62.9	43.3	28.5	4.5	t	q	3	n
63.5	40.1	34	0	p	s	3	n
68.4	34.5	22.7	0	r/w	q	4	n
42.4	36.5	27.1	4.3	g/t	s	3	n
50.3	46.1	31.4	0	u	s	3	n
56.1	27.5	20.7	3.6	w	q	3	n
64	44.3	27.7	0	t	s	3	n
25.9	25.4	6.6	0	e	s	3	n
63	30.1	16.6	0	e	s	3	n
77.1	52.7	54.3	0	br	s	3	n
95	65.5	31.7	0	br	s	3	n
61.8	47.6	45.3	0	br	s	3	n
69.3	58.5	20.7	0	b	m	3	n
67.7	44.2	41.8	0	u	s	3	n
71.3	49.4	34.2	0	u	s	3	n
84.2	42.1	22.9	0	u	s	3	n
61.2	43.5	22.1	0	u	s	3	n
66.6	31.9	18.2	0	u	s	3	n
70.6	42.1	23.4	0	u	s	3	n
61.5	20	16.5	0	u	s	3	n
49.4	42.1	20.8	0	u	s	3	n
57.1	37.7	29.8	0	u	s	3	n
50.8	40.9	30.6	0	u	s	3	n
74.4	38.7	28.4	0	u	s	3	n
53	37.4	22.4	0	br	s	3	n
53.9	17.9	13.3	2.6	u	s	3	n
47.4	28.6	21.6	0	u	s	3	n
51.7	29.7	31.1	2.2	t/w	q	4	n
47.5	37.9	31.2	2.1	g/t	s	3	n
58.6	35.9	23.3	0	w	q	3	n
42	37.5	33.2	2.4	w	q	3	n
58.8	45.7	18.4	4	g/t	s	3	n
50.4	40	27	0	t	s	3	n

37.6 29.9 11.4 1.3 w q 3 n

### Conococheague Creek

A-axis	B-axis	C-axis	avg. rind thickness	color	rock type	weathering	fabric
144.1	86.1	61.8	0	w	q	2	n
100.7	78.5	51.1	2.8	w	s	3	n
103	58	41.9	3.1	g	q	3	n
120.1	77.6	45.8	2.3	w	q	3	n
89.2	87.8	37	2.7	t	s	3	n
133.5	90.5	54.8	0	r	q	2	n
92.9	66.6	59.5	1.1	t	q	3	n
116.8	74.1	27.4	0	g	q	3	n
107.7	74.6	31.5	1.1	t	s	3	n
114	91.4	30	2.6	w	q	3	n
103.4	64.4	47.9	0	t	s	4	n
110.9	91.1	29.9	0	w	q	2	n
117.4	69.4	44.4	0	t/u	q	2	n
92.8	75.2	43.4	4	g	q	3	n
89	44.4	29.9	1.4	w	q	3	n
68.1	56.9	38.2	0	u/t	q	4	n
82	62.3	52	1.5	g	m	3	n
106	45.7	20	0	t	q	5	n
85.5	38.5	36.1	1.8	w	q	3	n
85.4	65.5	35.6	0	w	q	3	n
67	46.1	22.9	1.5	w	q	3	n
77.5	59.4	22.8	1.5	t/w	q	3	n
70.2	50.9	24.3	2.1	t/b	s	5	n
55.2	48.5	41.4	3.6	w	s	4	n
74	49	38	0	r	s	4	n
75.6	37.5	23.3	2.9	w	q	3	n
63.7	56.6	29.5	2	w	q	3	n
83.8	35	20.1	1.9	p/w	q	4	n
72.2	47.6	36	0	g	q	4	n
63.4	50.3	20.7	1.1	t	q	3	n
59.8	35.5	10.2	0	g	m	3	n
64.6	38.4	34.5	0	t	q	4	n
62	51.1	25.1	1.8	t	q	3	n
49.2	36.5	22.7	0	w	q	2	n
65.1	39.1	20.7	0	w	q	2	n
50.8	38.4	20.8	0	w	q	3	n
53.5	32	19.7	1.7	w	q	3	n
52.3	36.5	18.3	3.6	w	q	3	n
47.2	41.9	25.8	0	w	q	2	n

56.8	37.1	23.2	1.5	w/t	q	3	n
44.2	37.2	15.2	2.6	w/t	q	3	n

### South Mountain Stream

A -axis	B-axis	C-axis	avg. rind thickness	color	rock type	weathering	fabric
128.9	86.1	79.4	0	w	q	2	n
149.9	119.8	71.2	0	u	s	2	y
123.1	118	74.3	4.2	p/u/t	s	4	y
154.6	73.1	56.6	3.2	r	s	3	n
127.3	98.6	70.4	0	t	s	3	n
112.2	98.2	68.2	6.7	w/u/r	s	3	n
106.2	69.8	61	4.2	w/r	s	4	n
114.6	93.8	44.2	2.1	e	m	3	n
100	59.9	45.1	0	w	s	3	n
126.9	100	50.9	0	t	s	4	y
85.9	44	40.9	0	p/t	s	3	n
155.5	72.4	65.2	1.9	t	s	3	n
154.6	79.5	41.6	4.2	w	s	3	y
100.6	64.3	44.6	1.75	p	s	4	n
128.4	73.6	49.4	3.5	g	q	3	n
79.1	58.1	49.2	2.1	t/w	q	3	n
110.2	67.6	29.9	0	w	q	3	y
114.9	83	53.1	0	t	s	3	n
93	88.1	36.5	0	t	s	4	y
110	63.7	36.3	4.9	w	q	3	y
104.3	80	43	2.9	w	s	4	n
93.4	74.7	35.9	2	p	s	4	n
94	60.1	48.6	0	t	s	3	n
84.7	52.9	30.8	1.7	g	q	3	n
73.1	50.7	41.5	3.6	g	q	3	y
75.3	57.7	49.5	0	t	s	3	y
78.1	77.3	27.8	2.5	w	q	3	n
76.3	60.8	22.7	4	g	q	3	y
72.6	53.6	40.1	2.4	p/t	q	3	n
94.9	60.6	35.5	0	w	q	3	y
77.5	68.1	27.6	0	t	s	3	n
62.5	59.7	25.1	0	w	q	3	y
57	39	24.5	4.1	w	q	3	y
42	23.9	17.1	3.8	t	q	3	n
63.1	38	13.2	0	p	q	3	n
47.5	23.9	21.3	0	t	q	3	n
27.2	22.2	16.1	0	g	m	5	n

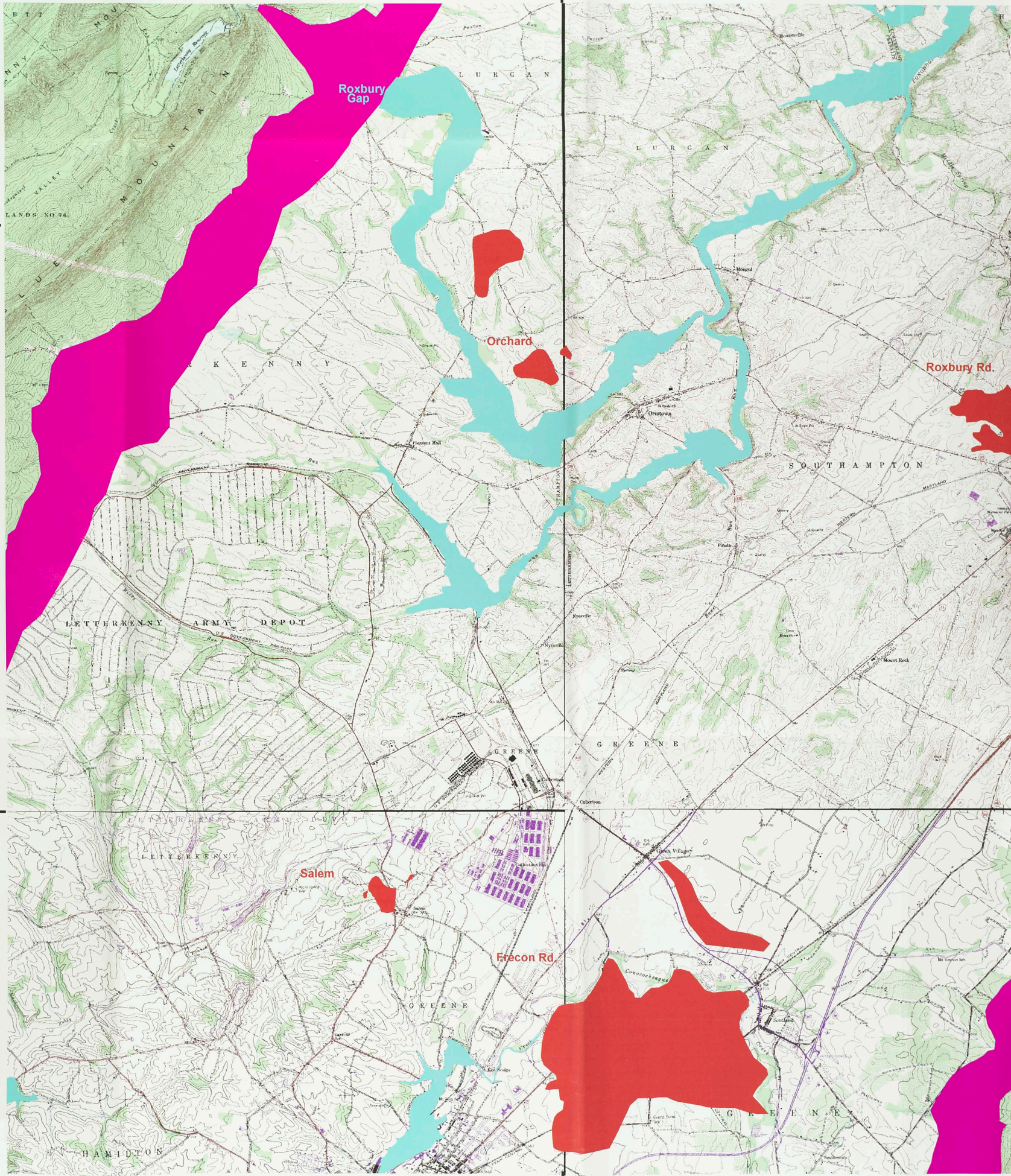
## Vita

Sarah M. Flanagan was born in Exeter, New Hampshire on October 4<sup>th</sup>, 1981 to Marguerite G. and John B. Flanagan and raised in Newbury, MA and Pound Ridge, NY. She graduated from Smith College, Northampton, MA in May 2003 with Honors in Geology. While at Smith she also attended Westchester Community College, Valhalla, NY in May of 2000, Cornell University, Ithaca, NY in July of 2001 and The University of Edinburgh, Scotland in the fall of 2001.

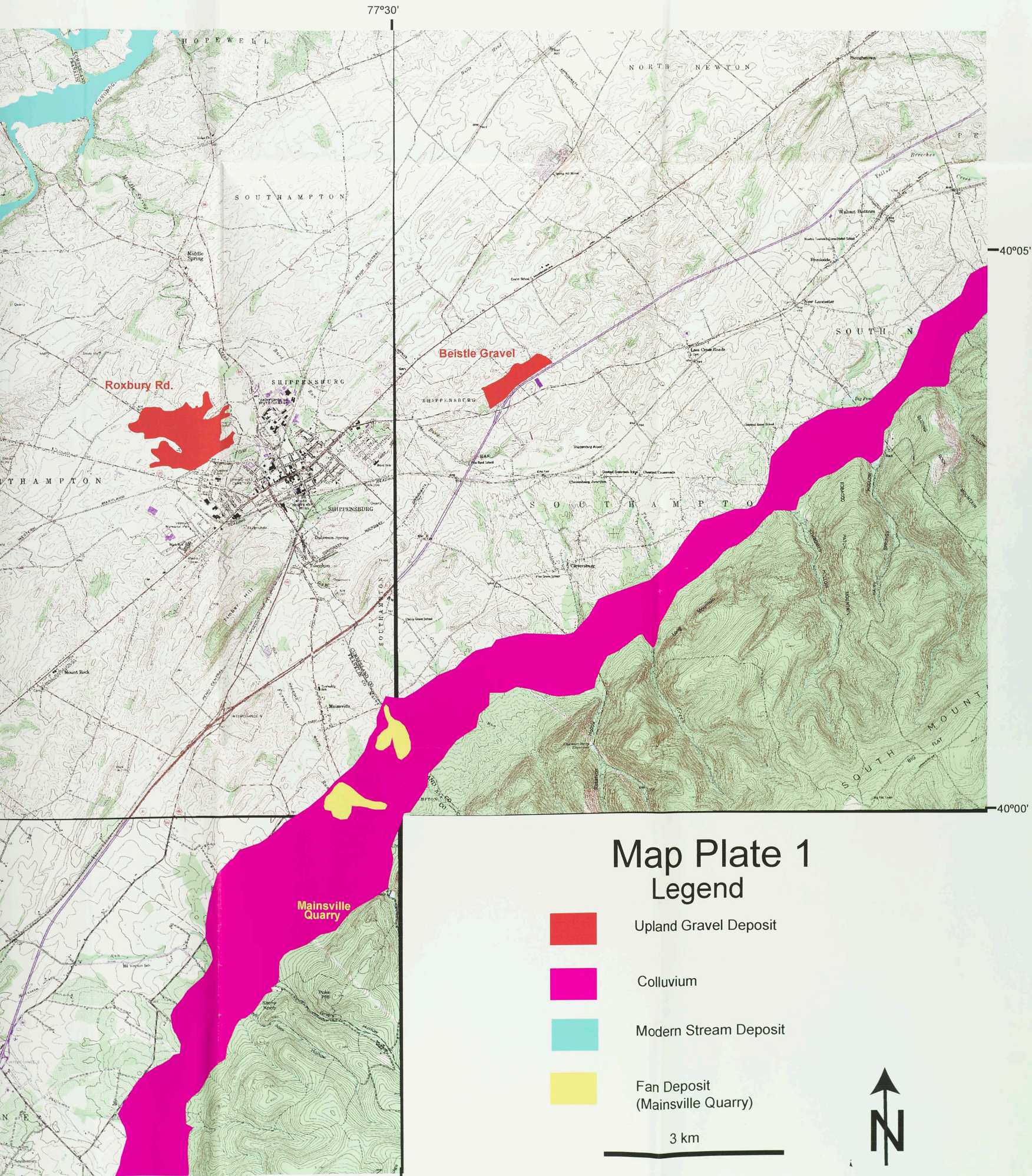
While at Lehigh University, she taught two laboratory sections of Introduction to Planet Earth.

77°37'33"

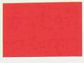
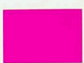

40°05'



77°37'33"



### Map Plate 1 Legend

-  Upland Gravel Deposit
-  Colluvium
-  Modern Stream Deposit
-  Fan Deposit (Mainsville Quarry)

3 km



77°30'

40°05'

40°00'

77°30'

**END OF  
TITLE**